Spectrochimica Acta Part A: Molecular and Biomolecular Spectroscopy 246 (2021) 119047

Contents lists available at ScienceDirect

Spectrochimica Acta Part A: Molecular and Biomolecular Spectroscopy

journal homepage: www.elsevier.com/locate/saa

Review Article

Recent development of chromogenic and fluorogenic chemosensors for the detection of arsenic species: Environmental and biological applications

Dipanjan Banik [a], Saikat Kumar Manna [b,*], Ajit Kumar Mahapatra [a,*]

[a] Department of Chemistry, Indian Institute of Engineering Science and Technology, Shibpur, Howrah 711103, West Bengal, India
[b] Department of Chemistry, Haldia Government College, Debhog, Purba Medinipur, Haldia 721657, West Bengal, India

ARTICLE INFO

Article history:
Received 2 August 2020
Received in revised form 29 September 2020
Accepted 2 October 2020
Available online 08 October 2020

Keywords:
Chromogenic and fluorogenic chemosensors
Arsenic
Environmental samples
Biological studies

ABSTRACT

Due to biological and environmental significance of highly toxic arsenic species, the design, synthesis and development of chemosensors for arsenic species has been a very active research field in recent times. In this review, we summarize recent works on the sensing mechanisms employed by fluorometric/colorimetric chemosensors and their applications in arsenic detection. Various types of sensing strategies can be categorized into six types including (i) chemosensors based on hydrogen bonding interactions; (ii) aggregation induced emission (AIE) based chemosensors; (iii) chemodosimetric approach (reaction-based chemosensors); (iv) metal coordination-based sensing strategy; (v) chemosensors based on metal complex displacement approach and (vi) metal complex as chemosensor. All these sensing strategies are very much simple and sensitive for use in the design of arsenic selective chromogenic and fluorogenic probes.

© 2020 Elsevier B.V. All rights reserved.

Contents

1. Introduction

One of the toxic metalloids responsible for ground water pollution is arsenic (symbol As, atomic number 33). The term arsenic originates from the Latin word *arsenicum* and from the Greek word *arsenikon* [1]. This ubiquitous, heavy element ranks 12th in human body, 14th in sea water, 18th in the universe and 20th in the earth's crust, in terms of the abundance of the elements [2]. In the Earth's crust the average concentration of arsenic is about 3 mg/kg and in sea water is about 1–2 μg/L [3,4]. This odourless element is a component of >245 minerals that are most commonly associated with sulphide containing ores along with gold, copper, lead, zinc, cobalt, nickel or other metals [5–8]. Generally, arsenic is discharged into the atmosphere by natural and anthropogenic activities. Weathering reactions, volcanic eruptions, marine

* Corresponding authors.
E-mail addresses: saikat.manna.chem@gmail.com (S.K. Manna), mahapatra574@gmail.com (A.K. Mahapatra).

https://doi.org/10.1016/j.saa.2020.119047
1386-1425/© 2020 Elsevier B.V. All rights reserved.

sedimentary rocks, fossil fuel, hydrothermal ore deposits and various biological activities are the most widely known natural sources of arsenic [9–12]. Arsenic may be released into the environment not only through geological processes but also through various anthropogenic activities, including leaching of arsenic containing rock, the smelting of arsenic bearing minerals, mining of sulphide ore,combustion of fossil fuels, well drilling, electrolyte processes, industrial waste, arsenic containing herbicides, pesticides and crop desiccants production, livestock feed additive, petroleum refining, leather and wood treatments, metals and alloys manufacturing, coalfly ash, ceramic manufacturing *etc*. [13–17]. Arsenic exists in several inorganic forms in the environment, such as -3 in AsH_3 (arsine), $+3$ in AsO_2^-, AsO_3^{3-} (arsenite), 0 (elemental arsenic) and $+5$ in AsO_4^{3-} (arsenate) [18–20]. Arsenic salts display a broad array of solubilities based on ionic strength and pH of the solution. Among the different oxidation states, inorganic forms of trivalent arsenic (As (III) or arsenite), prevalent in reduced atmospheres and pentavalent arsenic (As(V) or arsenate), dominant in oxygenated environments are the major species in natural water, especially in ground water [21–24]. Based on the chemical environment the ratio of As(V) to As(III) has been observed within the range of 10–100 [25–27]. Organo arsenic compounds such as monomethylarsonic acid (MMA), dimethylarsinic acid (DMA), trimethylarsine oxide (TMAO), arsenobetaine (AsB), arsenocholine (AsC) and arsenosugars are mainly found in aquatic organisms and are less important as they are less toxic or nearly non-toxic than inorganic arsenic [28]. However, As(III) has greater mobility in the environment and has been found to be 25–60 times more toxic to humans than As(V) [29,30]. Arsenic in groundwater has been a serious threat to plants, animals and human health [31,32]. In many countries, arsenic concentration in drinking water, irrigation water, various animal foods, agriculture products *etc*. has been found to be significantly higher than the WHO recommended allowable limits (10 ppb) for drinking water [33–36]. Inorganic arsenic can trigger both chronic and acute toxicity [37]. Chronic arsenic poisoning may cause respiratory problems, gastritis, colitis, anorexia, dyspepsia, loss of reflexes, weight loss, hair loss and abdominal pain [38–44]. Prolonged arsenic exposure *via* food or air causes a series of health hazards including cardiovascular diseases like ischemic heart diseases, hyperkeratosis, hyperpigmentation, hypertension, ventricular arrhythmia, atherosclerosis, disorders in the peripheral nervous and vascular systems, eczema *etc*. and it may even lead to the cancer of the liver, lung, kidney and bladder [45–50]. In addition, arsenic poisoning is also responsible for diarrhoea, loss of appetite, skin discoloration and lesions, feet and hand numbness, partial paralysis, blindness, diabetes, reproductive problems, leucomelanosis, melanosis, hallucinations, delirium and arsenicosis [51,52]. Arsenic is also genetically dangerous, as it prevents DNA damage from repairing [53]. Lipid metabolism [54] and glucose [55] uptake process is also inhibited by As(III). Moreover, As(V) compound stops the the Kreb's cycle by acting as a phosphate mimic and As (III) compound has a high affinity to thiol biomolecules resulting in the dysfunction of the main enzymes like pyruvate dehydrogenase [56,57]. Due to the very high toxicity of arsenic, the International Agency for Research on Cancer (IARC) and the U.S. Environmental Protection Agency (EPA) have classified arsenic as a group-1 human carcinogen [58]. Furthermore, United States Agency for Toxic Substances and Disease Registry (ATSDR) has placed arsenic as No. 1 on the hazardous materials priority list for several years [59]. Health concerns about arsenic toxicity have therefore motivated the development of effective methods (selective and sensitive) for real-time monitoring of arsenic in environmental and biological samples.

Up to now, several analytical techniques have been developed for the trace level determination of arsenic in environmental samples, such as cathodic stripping voltammetry (CSV), anodic stripping voltammetry (ASV), atomic absorption spectroscopy (AAS), atomic fluorescence spectroscopy (AFS), inductively coupled plasma-atomic emission spectrometry (ICP-AES), inductively coupled plasma mass spectrometry (ICP-MS), neutron activation analysis (NAA), energy dispersive x-ray fluorescence spectrometry (EDXRF), electro thermal atomic absorption spectrometry (ETAAS), graphite furnace atomic absorption (GFAAS), hydride generation-atomic fluorescence spectrometry (HGAFS), hydride generation atomic absorption spectrometry (HGAAS), capillary electrophoresis inductively coupled plasma mass spectrometry (CE-ICP-MS), hydride generative inductively coupled plasma atomic emission spectrometry (HG-ICP-AES) and high performance liquid chromatography-inductively coupled plasma mass spectrometry (HPLC-ICP-MS) [60–68]. These analytical methods although exhibit low detection limit but they have various disadvantages like need sophisticated and expensive equipment, complicated operational procedure, time consuming complex sample preparation suffers from false positive and false negative readings, interference problems, require trained professionals *etc*. [69–71]. Hence these methods are unsuitable for on-field and routine analysis especially for developing countries. However, the traditional colorimetric Gutzeit technique for arsenic detection is affordable and usable in field, but it exhibits false positive reactions and creates toxic by-products (arsine gas and mercury waste) [72]. Because of these complications, optical detection techniques (chromogenic and fluorogenic) have now emerged as an effective and preferable strategy for sensitive and quick detection of arsenic species attributable to their easy methodology, low cost, safe, user friendly, portability, selectivity, accuracy, repeatability, rapidity and the ability to monitor biological (*in vivo*/*in vitro*) and environmental specimens in real-time [73–78]. Therefore, many researchers have made significant efforts over the past few decades to develop chromogenic and fluorogenic chemosensors for the detection of arsenic ions.

To date, several reviews have been published on arsenic detection techniques such as electrochemical methods, biosensors, SERS methods, microfluidic technology and coupled technique [79–89]. In addition, optical detection techniques for arsenic have been recently reviewed [90,91]. However, the recent research findings on colorimetric and fluorometric arsenic chemosensors need to be summarized owing to the extensive attention and rapid development of this topic. In this review, we will concentrate mainly on the ongoing advancement of colorimetric and fluorometric chemosensors for the detection of arsenic in a careful and accurate way since the year 2012. The design approaches, sensing mechanisms, and applications of various arsenic selective chemosensors will also be discussed. All these chemosensors can be classified into six categories, according to their sensing strategies. These categories are (i) chemosensors based on hydrogen bonding interactions; (ii) aggregation induced emission (AIE) based chemosensors; (iii) chemodosimetric approach (reaction-based chemosensors); (iv) metal coordination-based sensing strategy (v) chemosensors based on metal complex displacement approach and (vi) metal complex as chemosensor (Fig. 1). Finally, we present our viewpoint on future progress which will be achieved in the development of novel probes for arsenic ions. We hope that this review will provide considerable help to the readers who wish to work in this area in the near future.

2. Arsenic sening mechanism

2.1. Chemosensors based on hydrogen bonding interactions

In the past few years, several chromogenic and fluorogenic chemosensors was designed and analysed for the selective detection of arsenic species using hydrogen bonding interactions strategy. Analyte binding to the donor site of the hydrogen bond or deprotonation of -OH, -NH moieties will cause a change in the optical property of the chemosensors. In this portion, we reported hydrogen bonding interactions based 'turn-on' fluorescent/colorimetric chemosensors for toxic arsenic species.

In 2013, Das et al. reported an antipyrine based fluorescent chemsensor for the detection of arsenate ($H_2AsO_4^-$) [92]. Upon gradual addition of $H_2AsO_4^-$ to the HEPES buffered (0.1 M) solution (methanol/water = 1:4, v/v, pH 7.4) solution of probe **1**, the emission intensity of the probe at 498 nm increased (quantum yield = 0.196). However,

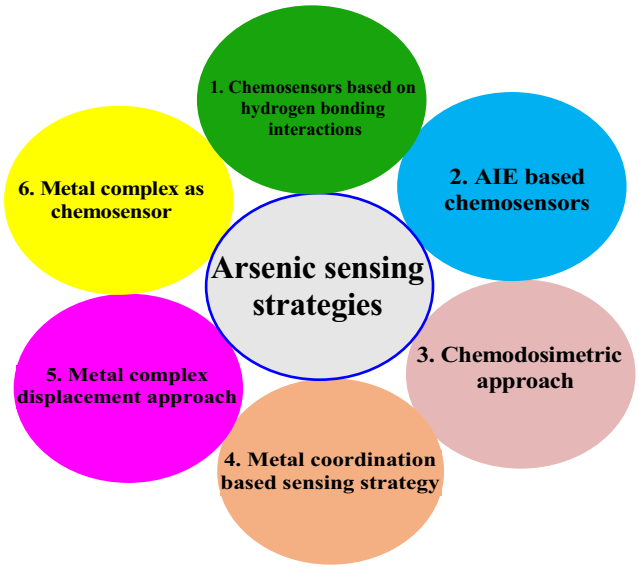

Fig. 1. Various arsenic sensing strategies.

other competitive anions including F^-, Cl^-, Br^-, I^-, N_3^-, NCO^-, NO_2^-, NO_3^-, SCN^-, CN^-, CH_3COO^-, SO_4^{2-}, ClO_4^-, and HPO_4^{2-} did not produce any dramatic fluorescence change, illustrating the high selectivity of the probe to $H_2AsO_4^-$. The authors suggested that such an enhancement of fluorescence was mainly due to the formation of strong hydrogen bonding between probe **1** and $H_2AsO_4^-$ ion. The binding constant between the **1** and $H_2AsO_4^-$ ion was calculated to be $8.9 \times 10^3\ M^{-1}$. The estimated detection limit of the probe was found to be $3\times\ 10^{-6}$ M. Moreover, the probe was used to detect intracellular $H_2AsO_4^-$ ion in contaminated living cells (Fig. 2).

Another interesting fluorescent chemosensor **2** for the sensing of arsenate was reported in 2014 by Das and coworkers [93]. Probe **2** was weakly non fluorescent due to Twisted Intra-molecular Charge Transfer (TICT) and Photo Induced Electron Transfer (PET) mechanisms from nitrogen centers of amino thiophenol moieties to diformyl phenol unit. However, in presence of $H_2AsO_4^-$, a 19-fold fluorescence enhancement at 532 nm was observed. The arsenate prompted fluorescence spectral changes were due to the intramolecular hydrogen bonding supported conversion of Twisted Intra-molecular Charge Transfer (TICT) to Planar Intra-molecular Charge Transfer (PICT) process (Fig. 3A). Detection limits of probe **2** for $H_2AsO_4^-$ was calculated to be 0.001 μM and other competitive analytes did not exhibit any fluorescence enhancement. A 1:1 (probe **2**: $H_2AsO_4^-$) binding stoichiometry was estimated by Job's plot analysis, and the association constant of probe **2** with $H_2AsO_4^-$ was found to be $1.35 \times 10^6\ M^{-1}$. The probe was applied to sense intracellular arsenate in various cells including *Candida albicans*, *Bacillus* sp. and pollen grains of *Tecomastans*. Again, with a fluorescence microscope, probe was able to monitor intracellular arsenate in microbes grown in arsenate affected drinking water samples (Fig. 3B). However, the authors prepared a **2**-embedded Merrifield polymer that was able to remove toxic arsenate from drinking water.

The same research group devised another turn-on fluorescent probe for $H_2AsO_4^-$ [94]. The absorption spectra of free probe 3 displayed a broad peak at 342 nm which decreased upon gradual addition of arsenate and subsequently a new peak at 412 nm was formed. Initially, the probe 3 showed very weak fluorescence at 530 nm owing to the PET process from N centres of the pyridyl moieties to the diformyl phenol unit but was converted to highly green fluorescent compound (3b) with 13.4-fold enhancement in the presence of arsenate as shown in Fig. 4. The increase in the emission intensity was due to the inhibition of the PET process from the free nitrogen centres upon arsenic binding and activation of intermolecular hydrogen bonding assisted CHEF (chelation-enhanced fluorescence) process. Probe 3 was found to bind with arsenate in a 1: 1 stoichiometric fashion, with the binding constant and the limit of detection $1.32 \times 10^4\ M^{-1}$ and 0.001 μM, respectively. Probe 3 was also highly selective to $H_2AsO_4^-$ among various anions examined. Additionally, cell imaging experiments established that this probe could be used to image arsenate in *Candida albicans* cells. Finally, the authors developed a probe 3 appended Merrifield resin polymer for the removal of arsenate from drinking water.

Chattopadhyay's group reported a new antipyrene based fluorescent chemosensor **4** for the selective detection of toxic AsO_3^{3-} ion in solution as well as in living cells [95]. Upon gradual addition of arsenate to the HEPES buffer (1 mM, pH 7.4; water: DMSO (v/v), 9:1) solution of **4**, led to a decrease in absorption band at 356 nm and a subsequently increase in peak at 428 nm with an isosbestic point at 380 nm. Probe **4** displayed a 9-fold increase in its emission intensity at 532 nm in the presence of arsenate, accompanied by a color change from colourless to green under UV-light. A strong intermolecular H-bonding between the probe and AsO_3^{3-} inhibited the PET process from nitrogen centres of the aminoantipyrene moieties to the diformyl phenol unit and produced CHEF which was responsible for the enhancement of the fluorescence intensity (Fig. 5). The sensing mechanism was confirmed by theoretical studies, ^{1}H NMR and mass spectroscopy. Job's plot implied that probe **4** generated a 1:1 complex with the AsO_3^{3-} and the binding constant was calculated to be $2.5267 \times 10^5\ M^{-1}$. The detection limit of

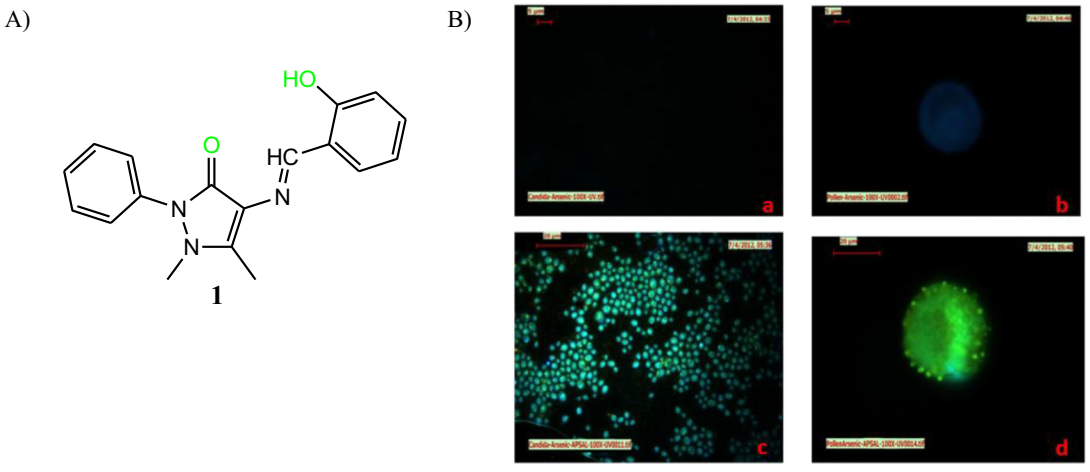

Fig. 2. A) Chemical structure of chemosensor **1**. B) Fluorescence microscopy images of *Candida albicans* cells (a & c) and pollen grains of *Allamandapuberula* (Aapocynaceae) (b & d): (a & b) cells treated only with $H_2AsO_4^-$, (c & d) cells treated with probe **1** + $H_2AsO_4^-$.
Reprinted with permission from Ref. [92] Copyright (2013) American Chemical Society.

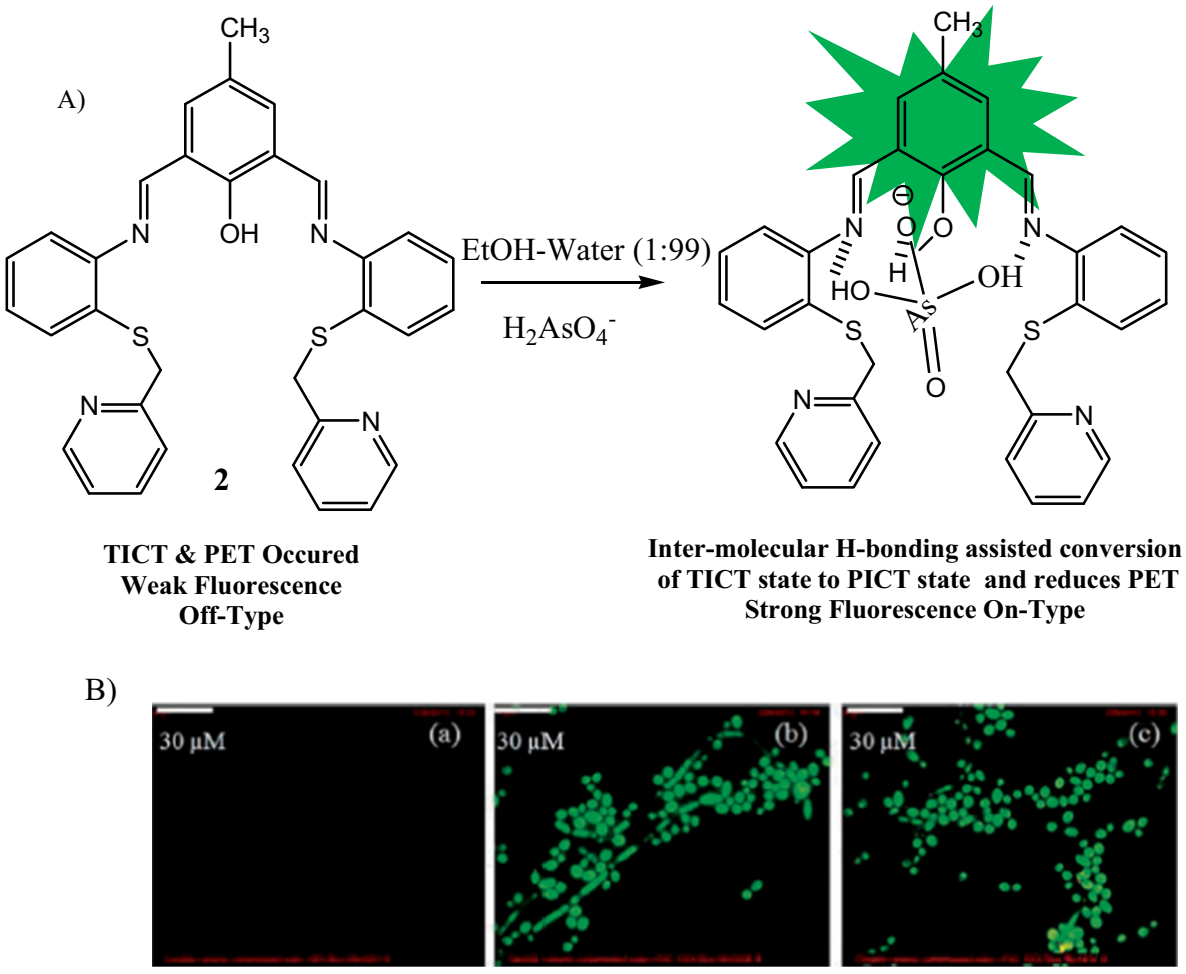

Fig. 3. A) Chemical structure of chemosensor **2** and its proposed binding interaction with $H_2AsO_4^-$. B) Fluorescence images of (a) microbes present in the drinking water samples; (b) and (c) microbes after treatment with Probe **2**.
Reproduced from Ref. [93] with permission of The Royal Society of Chemistry.

4 for arsenate was estimated at the ppb (4.12 ppb) level by using the fluorescence titration data. Notably, probe **4** could be employed to determine the trace level of arsenite ions in water samples.

Sirawatcharin and co-workers presented a simple colorimetric probe for the rapid and naked eye detection of As(III) in solution as well as in solid medium [96]. With addition of As(III) to the probe **5**

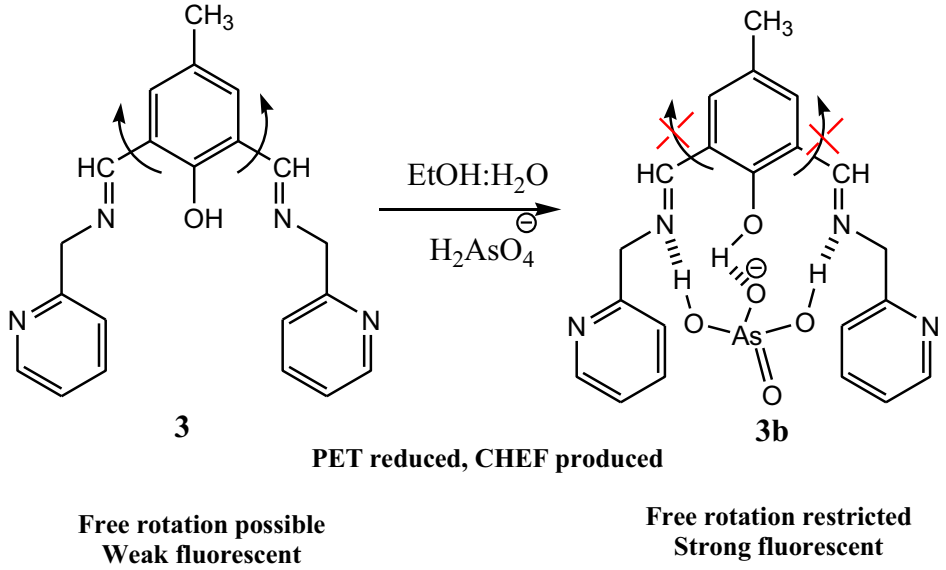

Fig. 4. Chemical structure of chemosensor 3 and its probable binding interaction with $H_2AsO_4^-$.

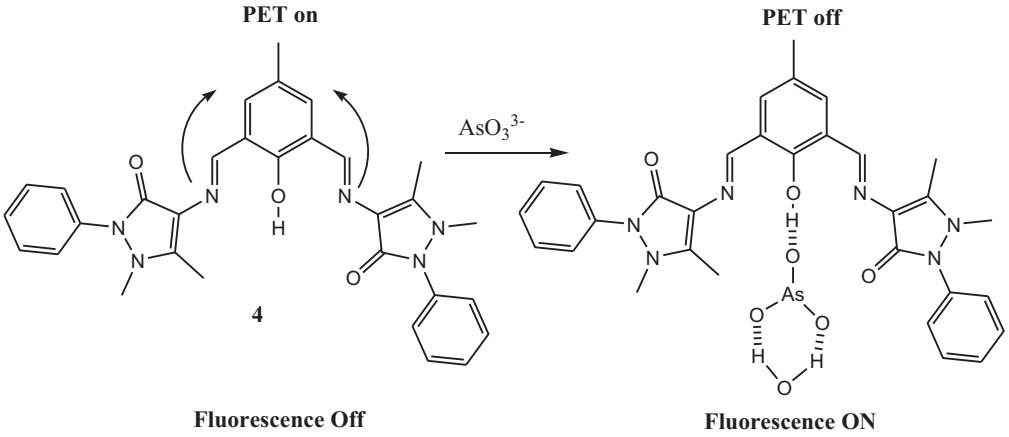

Fig. 5. Proposed binding interaction of chemosensor 4 with AsO_3^{3-}.

solution, the initial absorption peak of **5** red shifted from 509 nm to 632 nm, associated with the color change of the solution from orange to blue which was clearly noticeable to the naked eye. The color changes was due to the As(III)–mediated de protonation of the two –OH groups of the probe followed by the delocalisation of negative charge from donor to acceptor moiety as a shown in Fig. 6. The detection limits of the probe for As(III) were estimated to be 0.26 μM for UV–visible spectrometry, 25 μM for naked eye detection of BF_2-Curcumin solution and 30 μM for naked eye detection with BF_2-curcumin-coated resin. More importantly, the BF_2-curcumin-coated resin was successfully used to determine As(III) in water samples.

Das et al. reported another fluorescent probe **6** for the selective detection of arsenate in HEPES buffered (0.1 M, ethanol/water = 1/9, v/v, pH 7.4) solution (Fig. 7) [97]. In absence of arsenate, **6** exhibited an absorption band centred at 317 nm but in presence of arsenate **6** showed a new peak at 377 nm, signifying an important interaction between **6** and arsenate. In response to arsenate, probe **6** encountered 39 nm blue shifts (from 540 nm to 501 nm) in the fluorescence maxima which was due to H-bonding assisted AIEE and CHEF effect. The mentioned binding mechanism was supported by ^{1}H NMR spectroscopy. The binding stoichiometry was found to be 2:1 (probe **6**: $H_2AsO_4^-$) by the Job's plot and the binding constant was 1.38×10^5 $M^{-1/2}$. The probe **6** revealed a detection limit of 5×10^{-9} M for arsenate. Moreover, probe **6** selectively detect $H_2AsO_4^-$ over other common anions and was able to image intracellular $H_2AsO_4^-$ ion in *Candida albicans* cells. Additionally, Probe **6** was demonstrated for the trace level determination of arsenate in drinking water samples.

Gupta et al. synthesized two probes (**7** & **8**) for the selective colorimetric detection of arsenite ion (AsO_2^-) (Fig. 7) [98]. Upon addition of arsenite to the 5% H_2O-95% DMSO (v/v) solution of **7** & **8**, a significant color change from light yellow to pink for **7** and to dark pink for **8** occurred, accompanied by red shifts of 109 nm (from 395 nm to 504 nm) and 127 nm (from 407 nm to 534 nm), respectively in their absorption bands. Job's method suggested the formation of 1:1 complex between the probes and AsO_2^-. The formation of hydrogen bond between NH-proton of probes & AsO_2^- ion was the responsible for such color changes. Investigation also showed that **8** shows better response toward AsO_2^- than **7**, as it contains electron withdrawing $-NO_2$ group which increases the acidity of –NH proton. In addition, potentiometric experiments revealed that both probes could serve as an arsenite selective electrode and CGE (coated graphite electrode) exhibited better performance than PME (polymeric membrane electrode) in all parameters. The authors also demonstrated the use of these probes to determine arsenite ion in several water samples.

Recently, Sinha et al. developed a colorimetic and 'turn-on' fluorometric chemosensor **9** for the detection of PO_4^{3-} & AsO_3^{3-} *via* hydrogen bond assisted ESIPT mechanism (Fig. 7) [99]. When AsO_3^{3-} was added to the semi-aqueous solution (acetonitrile–water, v/v, 9/1, HEPES buffer, pH 7.2) of probe **9**, the initial absorption peaks at 312 nm and 368 nm gradually decreased, followed by an increase in a new band at 458 nm. The color of the solution changed from colourless to dark yellow, allowing naked detection of AsO_3^{3-} by probe **9**. Moreover, AsO_3^{3-} induced intense yellow emission appeared at 560 nm (35-fold enhancement). The main reason behind changes in the probe's optical nature in presence of AsO_3^{3-} was attributed to the strong hydrogen bonding between the AsO_3^{3-} ion and –NH/–OH group of the probe **9**, which can induce ESIPT-emission with structural rigidity enhancement. The Job's plot and mass spectroscopy confirmed the 1:1 stoichiometry of the complex formed between probe and AsO_3^{3-}. The binding constant for AsO_3^{3-} determined by Benesi-Hildebrand plot was found to be 1.0×10^5 M^{-1}. The limit of detection of chemosensor **9** for the AsO_3^{3} was 15 nM. Furthermore, this probe was employed for the analysis of ground water.

Ali and co-workers described a di-oxime based turn-on blue emission fluorescent chemosensor **10** for the detection of arsenate and

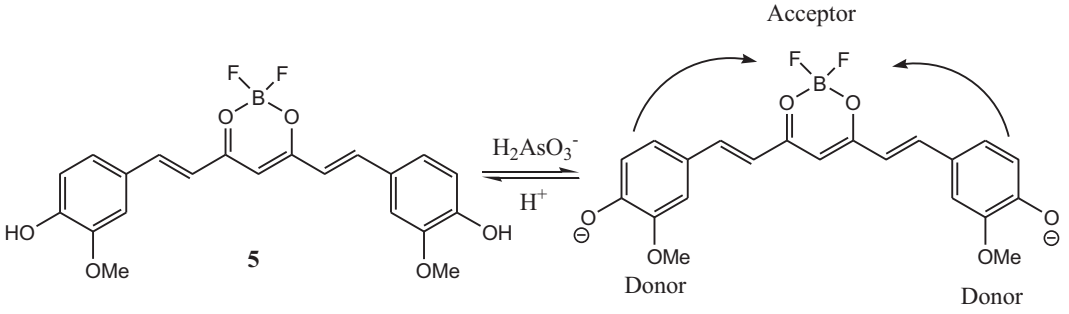

Fig. 6. Sensing mechanism of chemosensor 5 for AsO_3^{3-}.

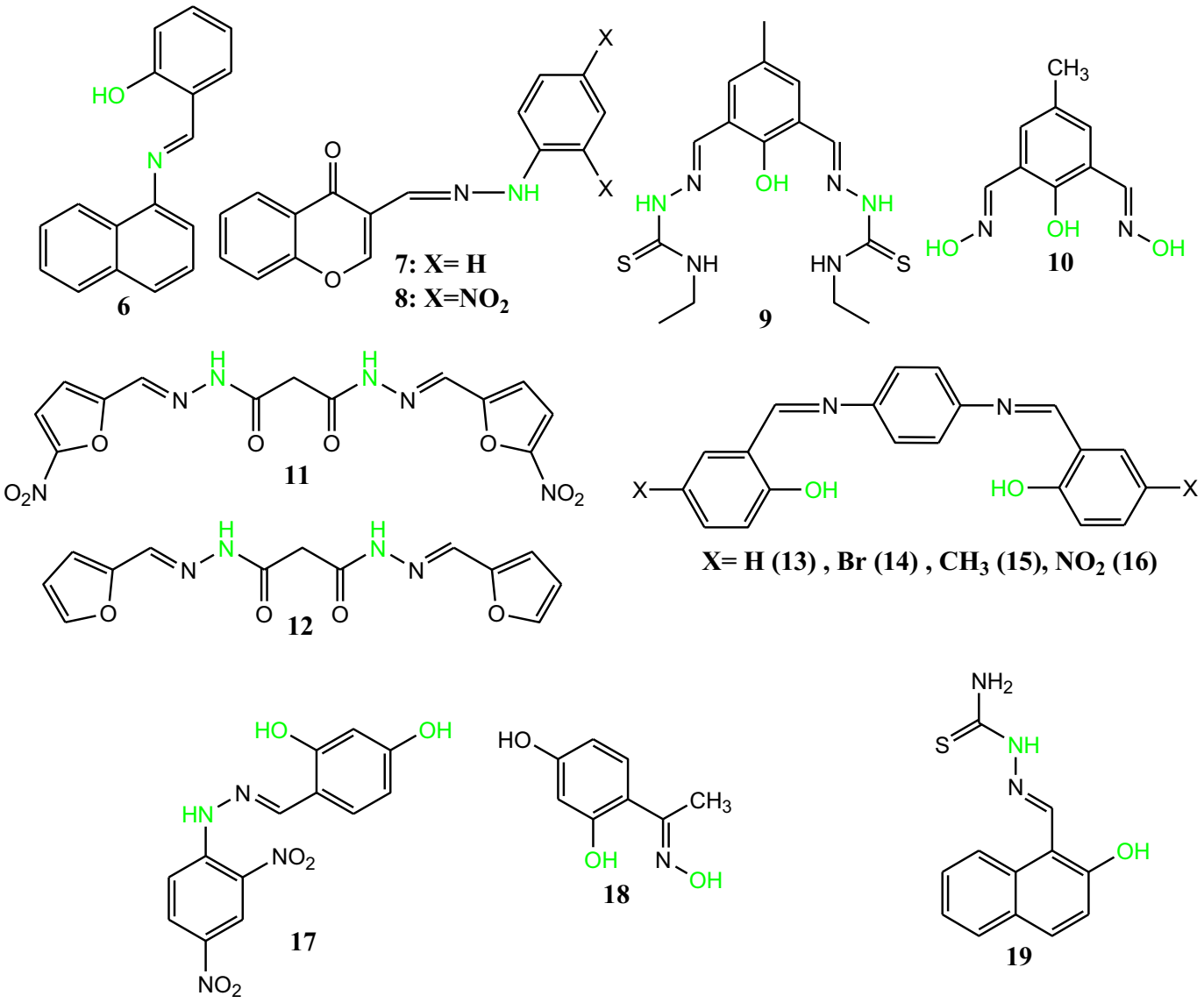

Fig. 7. Chemical structures of chemosensors **6**–**19**.

arsenite in pure aqueous medium at pH 7.24 (10 mM HEPES buffer, μ = 0.05 M, NaCl) (Fig. 7) [100]. The fluorescence intensity of probe **10** was enhanced 5-fold at 476 nm and 2-fold at 460 nm in the presence of AsO_2^- and $H_2AsO_4^-$, respectively, while no significant fluorescence enhancement observed with other cations, anions and organic arsenic species. The fluorescence quantum yield of **10** increased from 0.031 to 0.055 for H_2AsO_4- and to 0.078 for AsO_2^- and this was due to intermolecular H-bonding interaction between probe **10** and analytes (arsenate and arsenite). According to the mass spectroscopy and Job's method, the binding stoichiometry between probe **10** and analytes was 1: 1. The formation constant were found to be $(2.80 \pm 0.58) \times 10^4\ M^{-1}$ for AsO_2^- and $(2.03 \pm 0.97) \times 10^5\ M^{-1}$ for $H_2AsO_4^-$. The estimated detection limit of the probe was determined to be 1.32 μM and 0.23 μM for AsO_2^- and $H_2AsO_4^-$ respectively. The probe **10** exhibits good cell permeability, low cytotoxicity, and was successfully used to monitor intracellular AsO_2^- and $H_2AsO_4^-$ in HepG2 cells.

Singh et al. reported two malonohydrazide based colorimetric probes (**11** & **12**) for the detection of F^-, AcO^-, AsO_2^- and maleate ion (Fig. 7) [101]. The absorption spectrum revealed that upon addition of AsO_2^- ion to the probe **11** solution resulted in a bathochromic shift of 145 nm of the absorption band (isosbestic point at 434 nm), followed by a colorimetric change from pale yellow to wine red. Similarly, in presence of AsO_2^- ion, probe **12** induced an apparent bathochromic shift of 131 nm (isosbestic point at 415 nm), associated with a clear visible color change from pale yellow to orange red. The difference in absorption spectrum for the two probes was attributed to their molecular structure. The presence of two $-NO_2$ groups facilitates the formation of strong hydrogen bond between sensor **11** and AsO_2^- ion, that's why sensor **11** showed large bathochromic shift compared to sensor **12** The binding constants of sensor **11** and **12** were found to be $6.9 \times 10^5\ M^{-1}$ & $3.8 \times 10^5\ M^{-1}$ respectively. The binding stoichiometry was found to be 1:2 (sensor: AsO_2^-) in case of sensor **11** and 1:1 (sensor: AsO_2^-) for sensor **12**. The lowest detection limit for sensor **11** was 0.154 ppm (4.97 μM) whereas for sensor **12** was 0.99 ppm (6.52 μM).

Wang et al. developed a series of fluorescent probes, **13**–**16**, for the selective detection of As(V) (Fig. 7) [102]. In presence of As(V), the probe **13** displayed a sharp increase in the absorption peak at 270 nm and a slight decrease at 370 nm along with the formation of a new peak at 430 nm which increased significantly upon gradual addition of As(V). The color of the probe **13** solution was then changed from colourless to yellow which was clearly noticeable to the naked eye. Initially, probe **13** showed weak fluorescence at about 550 nm in DMF/

Water (v/v, 4:6) solution whereas the emission intensity increased greatly (91-fold) with the addition of As(V) and the fluorescence color changes from colourless to green under UV lamp. The binding stoichiometry of **13** and As(V) was found to be in the molar ratio of 1:2 (probe: analyte), as illustrated from the analysis of Job's plot and the binding constant was calculated as 4.26×10^4 M^2 from fluorescence titration spectra. This probe displayed a very low detection limit of 0.88 ppb. The change in fluorescence intensity was mainly due to intermolecular H-bonding assisted conversion of TICT (twisted intramolecular charge transfer) to PICT (planar intra-molecular charge transfer) and inhibition of PET process from the nitrogen centres. On addition of As (V), both probes (**14** & **15**) also showed a gradual increase in absorption bands at 238 nm and 375 nm respectively. Again, on gradual addition of As(V) to the DMF solution of both probes, there was an enhancement in the emission intensities at 550 nm. Job's plot revealed that both probes were bound with As(V) with a 2:1 (probe: analyte) stoichiometry and binding constants of **14** & **15** were estimated as 1.93×10^4 $M^{-1/2}$ & 1.79×10^4 $M^{-1/2}$ respectively. The detection limit of **14** & **15** were found to be 1.90 ppb & 2.42 ppb respectively. Investigation found that all the three probes were able to detect As(V) selectively over other anions and cations and even As(III) did not show any interference with As (V) detection. Due to better selectivity and sensitivity over other probes, the **13** was used for detection of As(V) in real water sample. Again, Probe **16** did not cause an enhancement of fluorescence in the presence of As(V) and therefore was unable to act as an As(V) chemosensor.

By using the advantage of strong interaction of 2, 4-dinitrophenyl hydrazone with guest analyte *via* hydrogen bonding, Deepa et al. devised a cost effective and colorimetric probe **17** for sensing arsenite (As^{3+}) ion (Fig. 7) [103]. Probe was synthesized by simple Schiff base condensation of 2, 4-dihydroxybezaldehyde and 2, 4-dinitrophenyl hydrazine in ethanol solvent. In H_2O: DMSO (9:1, v/v) medium, upon gradual addition of arsenite (As^{3+}) ion to probe **17** was characterized by a decrease in absorption intensity, along with a red shift from 415 nm to 509 nm in the position of absorption maxima. Similarly, when investigated in H_2O: ACN (9:1, v/v) medium, the probe also exhibited red shift from 397 nm to 470 nm as well as by a decrease in absorption intensity in presence of arsenite (As^{3+}) ion. The probe **17** exhibited colorimetric response toward As^{3+} in DMSO and ACN medium with a color change from orange to purple and yellow to red, respectively, owing to As^{3+} induced hydrogen bonding and deprotonation of -OH protons of **17**. This binding interaction was also supported by NMR and FT-IR studies. The authors reported, *via* Job's plot analysis, that a 1:1 complex was formed between probe & As^{3+}. The binding constant and detection limit were found to be 3.96×10^6 M^{-1} and 0.35×10^{-6} M, respectively. The probe was highly selective toward As^{3+} as no interference was observed by other metal ions like Cu^{2+}, Hg^{2+}, Fe^{3+}, Fe^{2+}, Zn^{2+}, Pb^{2+}, $Ni^{2+}$and Co^{2+}.

Ali et al. synthesized an oxime based fluorescent probe **18** that gave turn-on blue fluorescence response in the presence of arsenate ion ($H_2AsO_4^-$) based on the intermolecular H-bonding interaction between **18** and $H_2AsO_4^-$ ion (Fig. 7) [104]. The Job's plot analysis demonstrated a 1:1 type complex formation between probe **18** & $H_2AsO_4^-$. Moreover, the proposed intermolecular hydrogen-bonding interaction was supported by ^1H NMR studies. The binding constant of **18** for $H_2AsO_4^-$ was in the range of 10^4 M^{-1} with a limit of detection (LOD) of 29 μM. Probe **18** presented high selectivity toward $H_2AsO_4^-$ ion over other relevant anions and toxic metal ions. Probe **18** indicated negligible cytotoxicity and good cell permeability and could successfully monitor intracellular arsenate ion in HepG2 cells.

Singh and co-workers reported a naphthalene derivative **19** as colorimetric and turn-on fluorescent probe for the recognition of arsenite ion (AsO_2^-) and cyanide ion (Fig. 7) [105]. The addition of AsO_2^- led to increased fluorescence intensity at 495 nm and new absorption bands at 452 nm. Moreover, in presence of arsenate, a naked-eye visible color change from light yellow to dark yellow was observed in DMF: H_2O (HEPES buffer of 7.2 pH, 9:1, v/v) solution. The optical changes were attributed to the interaction between the probe (-OH and NH protons) and arsenite ion *via* deprotonation and hydrogen bonding. The binding interaction was also supported by NMR, DFT, ESI-MS and cyclic voltametry studies. The Job's plot revealed 1:1 binding stoichiometry between the probe **19** and arsenite ion with binding constant of 3.1×10^5 in DMF: Buffer medium and 3.2×10^5 in DMF:H_2O medium. The detection limit was found to be 66 nM in DMF: H_2O (9:1, HEPES Buffer) and 68 nM in DMF: H_2O (9:1). The probe was also used to determine unknown arsenite concentration in water and to analyse real water samples.

2.2. Aggregation induced emission (AIE) based chemosensors

Aggregation induced emission (AIE) is a distinctive fluorescence concept which was coined by Tang et al. in 2001 [106]. Generally, AIE probes displays weak fluorescence in solution state, but because of the restricted intramolecular rotational freedom, they become highly fluorescent in the aggregate state. This AIE phenomenon has been used in recent years for the development of fluorescent probes. Tetraphenylethylene (TPE) has attracted extensive interest among various AIE based fluorophores because of its excellent photophysical properties and good structural flexibility.

Baglan et al. developed a cystine fused TPE (tetra phenyl ethene) based 'turn-on' fluorescent probe **20** for the selective detection of toxic As^{3+} in aqueous media [107]. Here, AIE mechanism for fluorescence is involved in the sensing process. The authors suggested that the binding between the free –SH group of cysteine moiety and As^{3+} induced the formation of symmetric $As(cysTPE)_3$ and resulted in an increase in fluorescence due to the nature of AIE affects (Fig. 8). In aqueous solution, probe **20** shows very weak fluorescence but a strong AIE-emission band at 470 nm was observed, indicating the formation of As-complex. The detection limit of probe **20** for As^{3+} was calculated at the ppb level (0.5 ppb), that is below the WHO recommended standard limit. Moreover, various metal ions including As^{5+} did not induce any obvious fluorescence changes.

In 2017, Tian and co-workers designed and synthesized a carbazole based AIE active chemosensor for ultra-sensitive and selective detection of As^{3+} in THF–water mixtures (v/v, 3/7) (Fig. 9) [108]. Their investigation reveals that As^{3+} binds with free –SH group present in cysteine moiety of the probe **21** and led to a fluorescence enhancement at 455 nm due to AIE effect. The Job's plot suggested that the probe **21** formed a 1:3 complex with As^{3+}. This stoichiometric result was also supported by ^1H NMR titration and mass spectrometric analysis. The emission intensity of probe **21** displayed a good linearity with the As^{3+} concentration in the range of 0 to 120 ppb and the detection limit was found to be 1.32 ppb. To determine the selectivity of probe **21**, other competitive analytes such as As^{5+}, Ni^{2+}, Mn^{2+}, Co^{2+}, Pb^{2+}, Cd^{2+}, Cu^{2+}, Al^{3+}, Hg^{2+}, Fe^{2+}, Cr^{3+}, Fe^{3+} and anions were also examined under the similar experimental conditions and found that all these interfering species did not exhibit any noticeable changes in fluorescence spectra. Additionally, probe **21** was successfully employed to detect As^{3+} in real water samples.

2.3. Chemodosimetric approach (reaction-based chemosensor)

In recent years, considerable efforts have been made to develop the reaction-based chemosensors *i.e.* chemodosimeters for the detection of several analytes. Chemodosimeters typically detect the target analyte *via* a highly selective and and irreversible chemical reaction. One example of arsenic chemodosimeters are discussed in this section.

Chemodosimeter **22**, described by Ezeh et al., was responsive to toxic As^{3+} ion based on ICT (internal-charge-transfer) mechanism [109]. In presence of As^{3+} ion, chemodosimeter **22** exhibited noticeable absorption changes (from 385 nm to 464 nm) and a 25-fold fluorescence enhancement (quantum yield = 0.101) at 496 nm. The sensing mechanism was suggested to take place through As^{3+} promoted

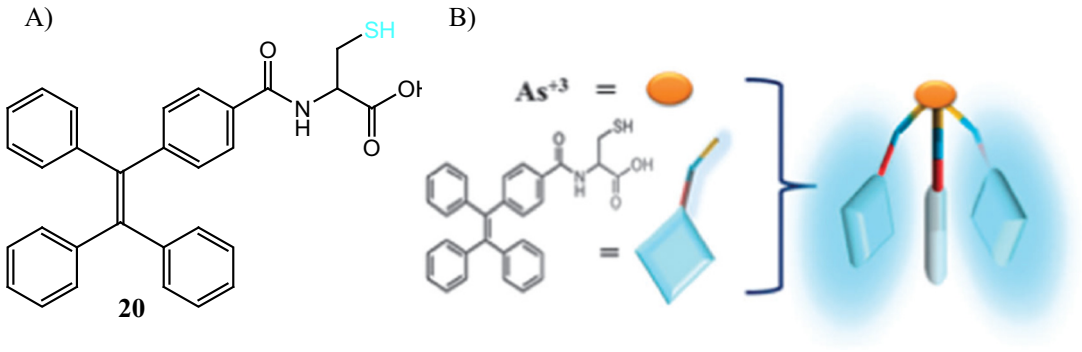

Fig. 8. A) Chemical structure of chemosensor **20**. B) Schematic view of the fluorescence activation of As(TPECys)$_3$. Reproduced from Ref. [107] with permission of The Royal Society of Chemistry.

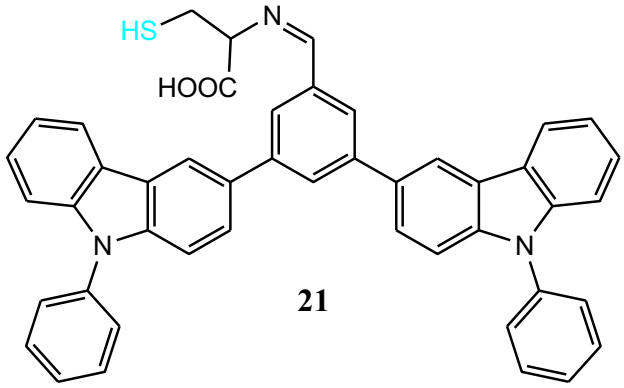

Fig. 9. Chemical structures of chemosensors **21**.

conversion of the non-fluorescent probe **22** to a highly fluorescent benzothiazole moiety (**22a**), as shown in Fig. 10. The probe **22** was highly sensitive to As^{3+} ion with a detection limit of 0.53 nM (0.24 ppb) which is much lower than the EPA instructed MCL value (10 ppb). The chemodosimeter **22** demonstrated a good selectivity for toxic As^{3+} ion over other biologically relevant metal cations (Na^+, Mg^{2+}, Ca^{2+}, Mn^{2+}, Fe^{2+}, Ni^{2+}, Zn^{2+}, Hg^{2+}, Pb^{2+} and Cd^{2+}) except that Cu^{2+} faintly responded to **22**. The proposed sensing mechanism was confirmed by ^{1}H NMR titration experiments.

2.4. Metal coordination-based sensing strategy

A highly selective, economical colorimetric chemosensor **23** was proposed and synthesized by Chauhan and co-workers for the rapid detection of arsenic (As^{3+}/As^{5+}) in DMSO/H_2O medium [110]. Upon addition of As^{3+}/As^{5+}, **23** demonstrated a large red shift (100 nm) of absorption band (from 480 nm to 580 nm), accompanied by a visual color change from light yellow to brownish orange color. The colorimetric changes were attributed to the formation of aggregated complex state **23**-As^{3+}/As^{5+} through N, S chelate of probe **23** as shown in Fig. 11. The Job's plot analysis revealed that a 1: 1 adduct was generated during complexation. Moreover, the detection limit for As^{3+} and As^{5+} were determined to be 7.2 and 6.7 ppb, respectively.

Banerjee et al. synthesized and reported a rhodamine based chromogenic and fluorogenic probe **24** for the highly selective and sensitive detection of As(III) in acetonitrile: HEPES buffer (4:1, v/v, pH 7.4) solution [111]. The absorption spectrum showed that upon gradual addition of As(III) to the organo aqueous solution of **24** resulted in an enhancement of the absorption peak at 525 nm, accompanied by a visible color change from colourless to reddish pink color. In absence of As(III), **24** was non-fluorescent due to closed spirolactam conformation of the probe, whereas the addition of As(III) led to an yellow emission at 555 nm upon excitation at 515 nm. The significant color and fluorescent changes were due to the formation of As(III)-induced ring opened spirocyclic structure (**24**a) of the probe **24** and this sensing mechanism was confirmed by ^{1}H NMR and FT-IR spectroscopy (Fig. 12). The binding constant of the probe for As(III) was calculated to be 0.33×10^6 M^{-1}. In addition, this As(III) sensing process was reversible upon addition of I^-. The probe **24** demonstrated superb selectivity toward As(III) and was effectively used for the detection of As(III) in several samples of wastewater with varying pH levels. Moreover, probe **24** was also employed to monitor As (III) in various cell lines including pollen grains of *Allamanda puberula* (Aapocynaceae), radiator plant (*Peperomia pellucida*), *Poecilia reticulata*, *Danio rerio*, and squamous epithelial cells.

Recently, Sutariya et al. described a fluorescent probe **25**, containing pyrene appended calix[4]arene moiety for sensing As^{3+}, Nd^{3+} and Br^- ions [112]. In presence of As^{3+}, probe **25** induced 17 nm red shift (from 261 nm to 278 nm) in the absorption spectra. Meanwhile, upon addition of As^{3+} to the mixed aqueous/organic solution of **25** (acetonitrile/

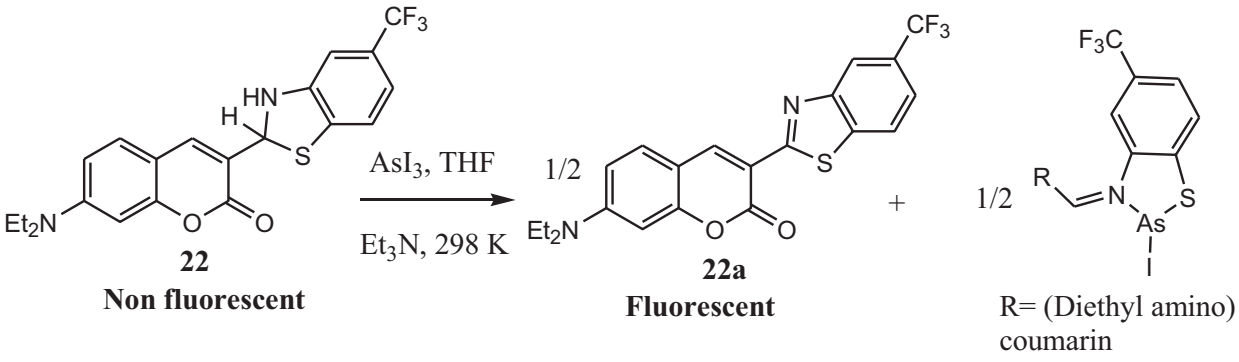

Fig. 10. Chemical structure of chemosensor **22** and its sensing mechanism for As^{3+}.

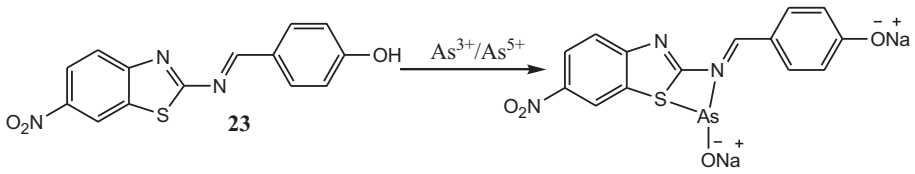

Fig. 11. Structure of chemosensor **23** and its proposed binding interaction with arsenic ions.

aqueous phosphate buffer (8: 2, v/v), pH = 7.2), a complete quenching of fluorescence (0.036-fold) was observed. The job's plot showed that a 1:1 complex was formed between the probe and As^{3+}, and the binding constant was estimated to be $7.842 \times 10^8\ M^{-1}$ (Fig. 13). This 1:1 stoichiometry was further confirmed by ESI–MS analysis. The detection limit for As^{3+} was evaluated to be 11.53 nM. The authors reported a low – cost and reusable paper-based sensing system for the detection of As^{3+} ions. Furthermore, the probe showed better results when detecting As^{3+} ions in wastewater samples compared with other reported As^{3+} detection methods.

A)

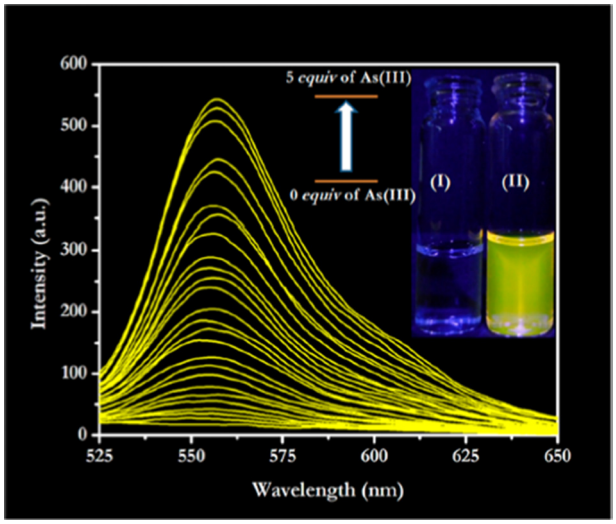

B)

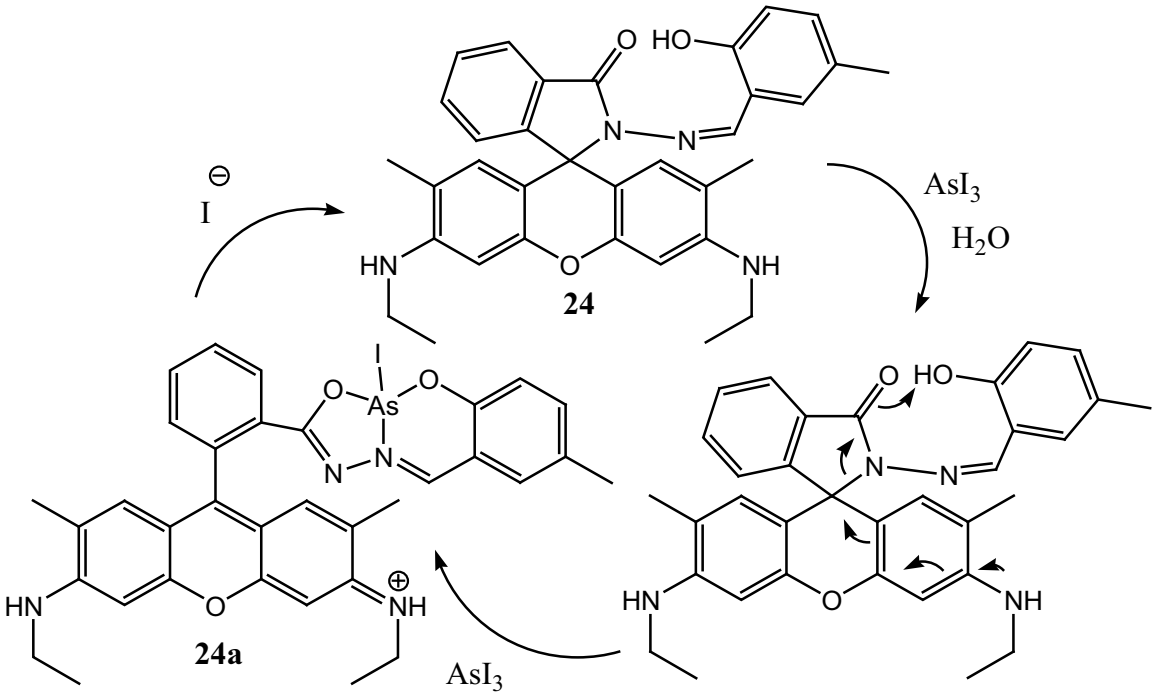

Fig. 12. A) Fluorescence emission spectra of probe in acetonitrile: HEPES buffer (4:1, v/v, pH 7.4) upon addition of As(III) in aqueous medium. Inset: Photographic images of (I) **24** and (II) **24** + As(III).
Reprinted with permission from Ref. [111] Copyright (2019) American Chemical Society. B) Chemical structure of chemosensor **24** and its sensing mechanism for As^{3+}.

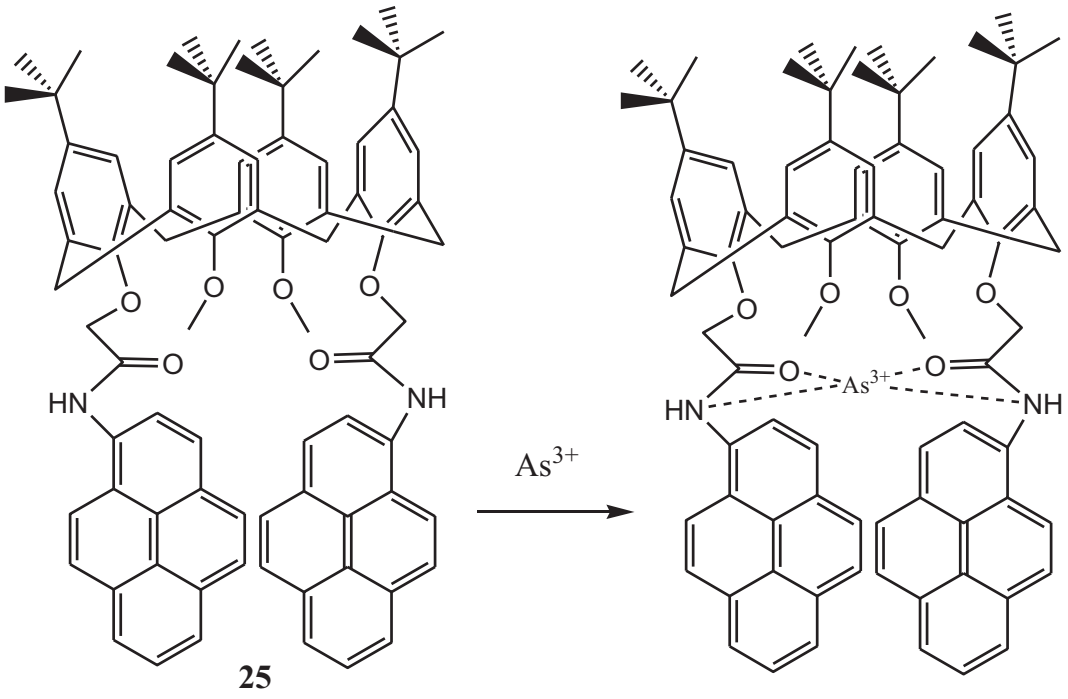

25

Fig. 13. Chemical structure of chemosensor **25** and its proposed binding mechanism with As^{3+}.

Park et al. reported a colorimetric sensor **26** for the selective detection of As^{3+} (Fig. 14) [113]. Large signal to noise (S/N) ratio intensity and a strong increase in the absorption spectra at 430 nm in presence of As^{3+} confirmed the interaction between sensor and As^{3+}. Cyclic voltammetry (CV) studies were performed to confirm the binding process. The sensor **26** presented a good selectivity for As^{3+} over other metal cations except that Cd^{2+} responded to the sensor in a negligible manner. Moreover, IR spectral study showed that $-NO_2$ group present in the sensor plays an important role during chelation with As^{3+} ion. Isothermal titration calorimetry (ITC) was also conducted to know about binding affinity and stoichiometry of the interaction. The detection limit was found to be as 31.8 nM. Furthermore, the sensor was successfully used to detect As^{3+} in various water samples including river and tap water.

2.5. Chemosensors based on metal complex displacement approach

Roy and co-workers reported a Al^{3+}-complex (**27**) probe for the detection of AsO_4^{3-} in CH_3OH–HEPES (7/3, v/v) solution [114]. Upon addition of Al^{3+}, free rhodamine derivative exhibited a noticeable colorimetic change from colourless to pink and remarkable enhancement of fluorescence intensity at 552 nm which was attributed to the formation of spirocyclic ring–opened Al^{3+}-complex. However, addition of AsO_4^{3-} to the *in situ* prepared Al^{3+}-complex solution led to the abstraction of Al^{3+} ion followed by the regeneration of the absorption and fluorescence of free rhodamine derivative (Fig. 15). Furthermore, other common ions such as Cl^-, Br^-, I^-, SO_3^{2-}, N_3^-, $HCOO^-$, CH_3COO^-, SO_4^{2-}, SO_3^{2-}, NO_3^-, $H_2PO_4^-$ and ClO_4^- did not exhibit any noteworthy changes in absorbance spectra as well as in fluorescence spectra of *in situ* prepared Al^{3+}-complex, indicating the selectivity for AsO_4^{3-}.

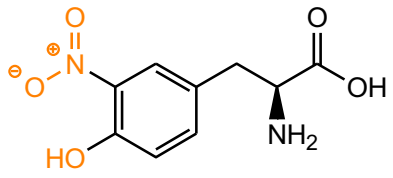

26

Fig. 14. Chemical structure of chemosensor **26**.

2.6. Metal complex as chemosensor

A metal complex based sensing strategy has also been employed for developing chemosensors for arsenic species.

The 2-(2-pyridyl) benzimidazole based Mn(II) complex **28** created by Das's group was employed for the turn-on fluorescence detection of $HAsO_4^{2-}$ (Fig. 16) [115]. Probe **28** demonstrated weak fluorescence at 440 nm (quantum yield $= 1.23 \times 10^{-2}$) in HEPES buffered (0.1 M) (methanol/water = 0.5/99.5, v/v, pH 7.4) solution, while emission intensity dramatically increased with the addition of $HAsO_4^{2-}$ (quantum yield $= 4.59 \times 10^{-2}$). Moreover, the color of the titration solution changed from colourless to blue under a UV light. The authors proposed that this fluorescence enhancement was ascribed to the formation of intermolecular hydrogen bonds between probe and $HAsO_4^{2-}$, resulting in greater molecular rigidity and lowered overall system entropy. Analysis of the results of a Job's plot stated that **28** was bound to $HAsO_4^{2-}$ with a 1:1 stoichiometry which was further confirmed by FT IR and ESI mass spectroscopy. From the fluorescence titration results, the binding constant for the 1:1 complex was calculated using the Benesi–Hildebrand equation and it was found to be $3.09 \times 10^3\ M^{-1}$. The large binding constant value clearly indicated that the probe **28** has high binding affinity for $HAsO_4^{2-}$ ion. Probe **28** demonstrated high sensitivity (Detection limit $= 1 \times 10^{-10}$ M) and selectivity for $HAsO_4^{2-}$ over other common anions (F^-, Cl^-, Br^-, I^-, N_3^-, NCO^-, NO_2^-, NO_3^-, SCN^-,CN^-, CH_3COO^-, SO_4^{2-}, ClO_4^- and HPO_4^{2-}) and was efficiently applied to image intracellular $HAsO_4^{2-}$ in various cells including *Allamandapuberula* cells and *Candida albicans* cells.

Dey et al. reported a water-soluble metal-organic complex (**29**) for the selective detection of inorganic As^{3+} in water medium (Fig. 17) [116]. Free probe displayed absorption and emission bands at 310 nm and 350 nm, respectively. However, the emission intensity of **29**

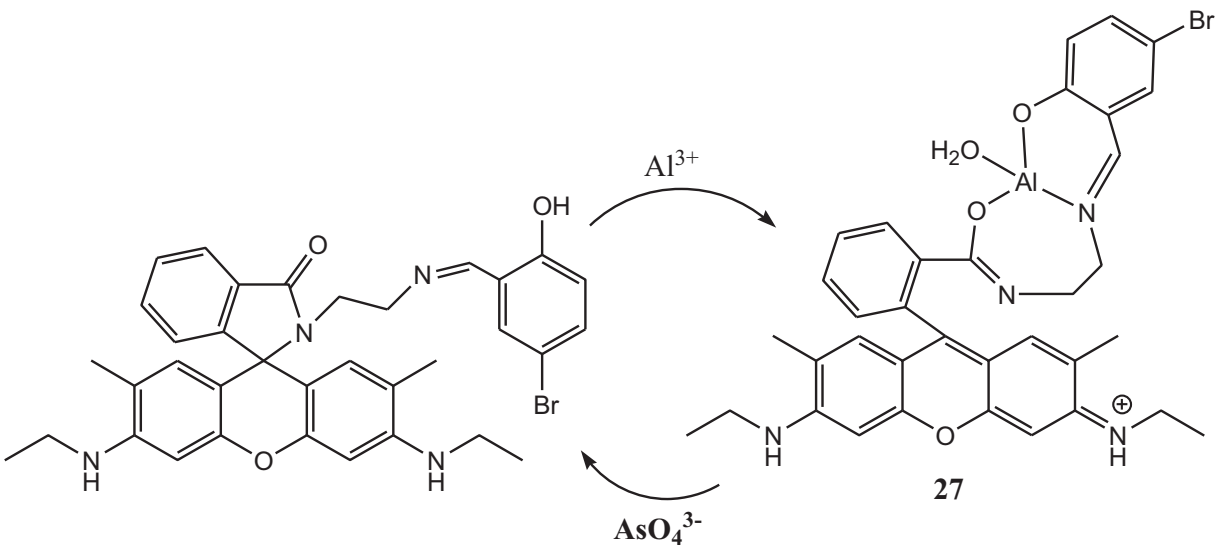

Fig. 15. Chemical structure of **27** and its sensing mechanism for AsO_4^{3-}.

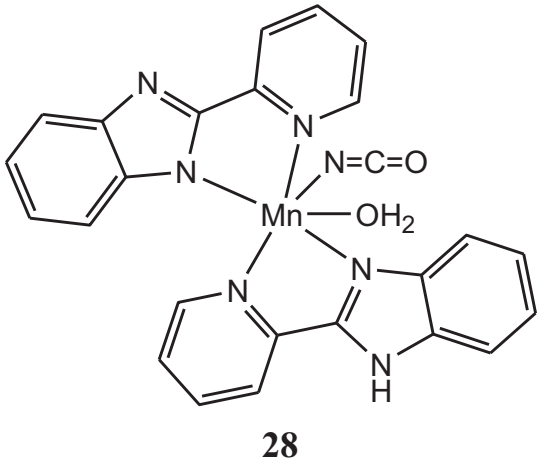

28

Fig. 16. Chemical structures of metal –complex chemosensor **28**.

increased with increasing As^{3+} concentration (from 49 pM to 4440 pM). The sensing mechanism was suggested to involve a weak non-covalent type interaction between As^{3+} and lone- pairs on free carbonyl oxygen atoms of carboxylate groups of the ligand, which was supported by both IR and ESI-MS spectra. The sensor **29** also demonstrated good selectivity toward As^{3+} over other metal ions including Li^+, Na^+, K^+, Ca^{2+}, Mg^{2+}, Co^{2+}, Ni^{2+}, Cd^{2+}, Hg^{2+}, Zn^{2+}, inorganic As^{5+} and organic As- species.

Dey and co-workers described a non-toxic and water soluble Cu(II)-complex based fluorescent probe **30** for the recognition of toxic inorganic As(III) as in water medium (Fig. 18) [117]. Initially, in aqueous solution, the free probe exhibited an emission and broad absorption band at 380 nm and 250 nm, respectively. However, upon non-covalent hydrogen bonding interactions between free carbonyl 'O' of the ligands of complex and $As(OH)_3$, an obvious enhancement of fluorescence intensity was observed. Investigation showed that the probe selectively detect As(III) over other As-species (organic arsenic-species (cacodylic acid) and inorganic As(V)-oxoanions) and metal ions (Li^+, Na^+, K^+, Ca^{2+}, Mg^{2+}, Fe^{2+}, Fe^{3+}, Mn^{2+}, Co^{2+}, Ni^{2+}, Cd^{2+}, Hg^{2+}, Zn^{2+}, Sn^{2+},

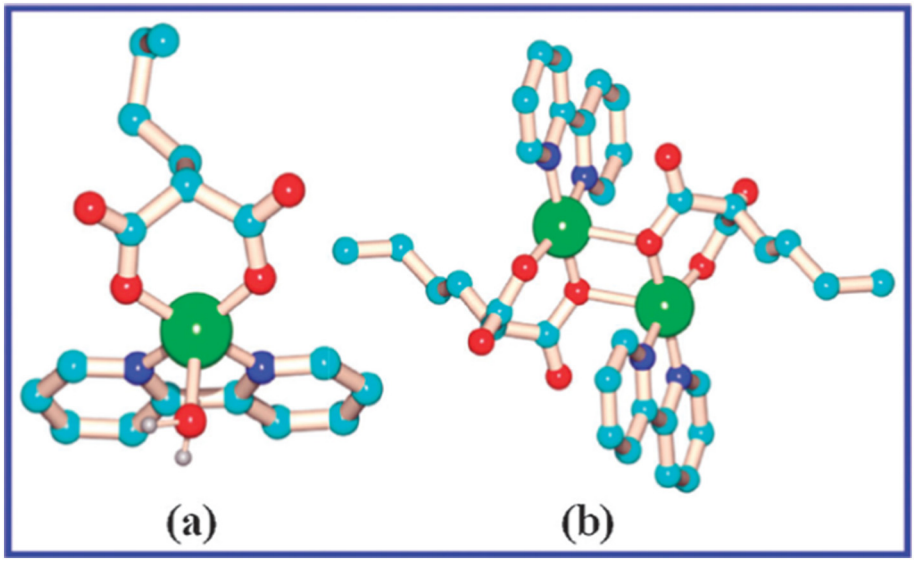

Fig. 17. Molecular diagram of the monomeric (a) and dimeric (b) units in **29** (here, C = cyan, N = blue, O = red, Cu = green). Reproduced from Ref. [116] with permission of The Royal Society of Chemistry.

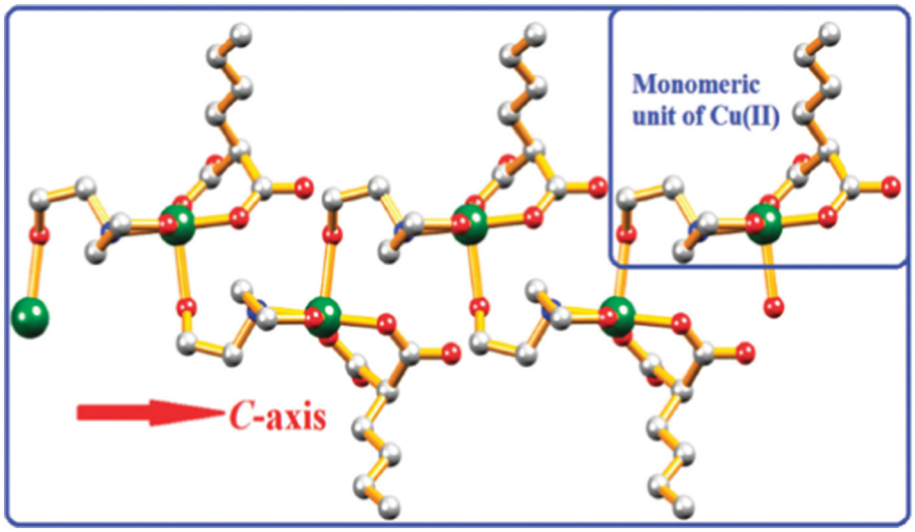

Fig. 18. One dimensional coordination polymer of Cu(II)-monomeric units (here, C = gray, N = blue, O = red, Cu = green) (**30**). Reproduced from Ref. [117] with permission of The Royal Society of Chemistry.

Sr^{2+}, Al^{3+}, Cr^{3+}, Bi^{3+} and Sb^{3+}) in the concentration range of femtomolar to micromolar (Detection limit = 49.75 fM) in water medium. The probe was nontoxic and the authors further successfully employed this probe to image As(III), for the first time, in various living system (on pollen grains of *Tecoma stans*; *Candida albicans* cells (IMTECH No. 3018) and *Peperomia pellucida* stem section).

Koner et al. designed and synthesized a small water-soluble probe (**31**) consisting of a perylene-Cu^{2+} complex with free carbonyl functional group to selectively detect As^{5+} ion in aqueous solution (Fig. 19) [118]. In aqueous solution (deionized water buffered with HEPES,1 mM, pH 7.2), the perylene -Cu^{2+}complex **31** showed weak fluorescent at 600 nm (quantum yield $\Phi = 0.032$) due to photoinduced electron transfer (PET) from the excited perylene to Cu^{2+}. But, when As^{5+} solution was added to the aqueous solution of **31**, a significant enhancement of fluorescence at 600 nm (quantum yield $\Phi = 0.344$) was noticed, which was attributed to the formation of perylene-As^{5+} complex *via* intermolecular H-bonding assisted chelation process. Due to higher binding constant of the perylene-As^{+5} complex (8.50×10^8 M^{-2}) than the perylene-Cu^{+2} complex (0.377×10^8), the perylene-Cu^{+2} complex undergoes a decomplexation process in presence of As^{5+} to form a new As^{+5} complex. Moreover, it was found that **31** has a detection limit of 26 nM. The probe **31** was found to highly selective and sensitive toward As^{3+} over competitive ions (F^-, Cl^-, Br^-, I^-, N_3^-, SO_4^{2-}, AcO^-, HCO_3^-, HSO_3^-, CN^-,Al^{3+}, Fe^{3+}, Cu^{2+}, Cd^{2+}, Ni^{2+}, Ag^+, Mn^{2+}, Zn^{2+}, Na^+, Mg^{2+}, Hg^{2+}, Co^{2+}, Pb^{2+}, Cr^{3+}, and As^{3+}) and was also used to detect As^{5+} in several real water samples. Furthermore, the probe **31** showed non toxicity and was successfully used for detection of intracellular As^{5+} in living HepG2 cells.

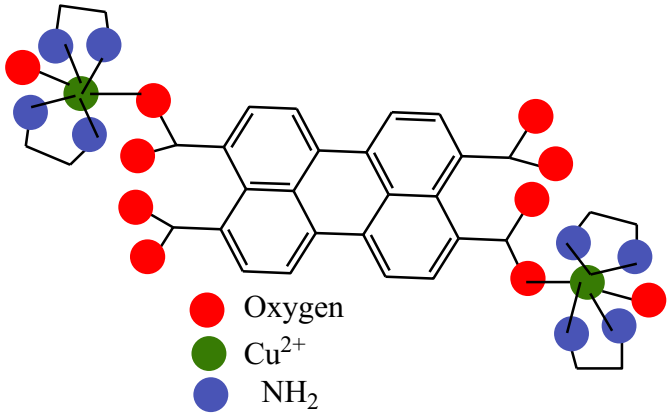

Fig. 19. Chemical structure of chemosensor **31**.

Das et al. reported a colorimetric and fluorometric AsO_2^- chemosensor based on the Mo(VI) involved complex **32**-Mo(VI) [119]. Chemosensor **32** showed great affinity for AsO_2^- over other competing ions and noticeable fluorescence enhancement (17-fold) in the presence of AsO_2^- ion. However, gradual addition of AsO_2^- to the DMSO/H_2O (4/1, v/v, pH 7.4) solution of **32** induced a 101-nm red shift in the emission spectrum along with 81-fold fluorescence enhancement and an associated color change from blue to bright green under UV lamp. This enhancement was due to the strong hydrogen bonding interaction between the complex and arsenite ion, which increases the rigidity and decreases the entropy of the system (Fig. 20). In presence of AsO_2^-, chemosensor **32** displayed two absorption bands at 367 nm and 477 nm, with color varying from yellow to orange.The mass spectrum and Job's plot analysis revealed that the stoichiometry between complex and AsO_2^- was 1:1. The binding constants of chemosensor **32** with Mo(VI) and AsO_2^- were calculated as 4.21×10^5 M^{-1} and 6.49×10^4 M^{-1}, respectively. The AsO_2^- detection limit for this probe was recorded as 1.2×10^{-10} M. This complex was effectively implemented to image intracellular AsO_2^- in A549 cells. This complex was successfully employed to determine AsO_2^- in real water samples. The authors again used this complex to remove AsO_2^- ion by solid-phase extraction method from environmental samples.

Dey group designed a nontoxic water soluble fluorescent Co(II) complex probe (**33**) for the selective detection of toxic inorganic As (III) in micro molar range in water medium (Fig. 21) [120]. This complex showed high selectivity and sensitivity toward As(III) in terms of enhancement in emission intensity without any interference from inorganic As(V) oxo-anions, organic arsenic species like cacodylic acid and other ions (Li^+, Na^+, K^+, Ca^{2+}, Mg^{2+}, Fe^{2+}, Mn^{2+}, Cu^{2+}, Ni^{2+}, Cd^{2+}, Zn^{2+}, Sn^{2+}, Cr^{3+}, Sb^{3+}, Pb^{2+}, F^-, Cl^-, Br^-, SO_4^{2-}, N_3^-, BF_4^-, Cr(VI)-oxo anions and PO_4^{3-}). This enhancement was due to non-covalent binding interactions between $As(OH)_3$ and free carbonyl oxygen sites of Co(II) complex probe as supported by ESI-MS and IR spectral studies. The detection limit was estimated to be 0.49 μM. Moreover, the complex had good biocompatibility and low cytotoxicity that allowed it to be employed for the intracellular tracking of inorganic As(III) in both arsenic resistant bacteria (*Bacillus aryabhattai*) and arsenic non resistant bacteria (*Bacillus subtilis*).

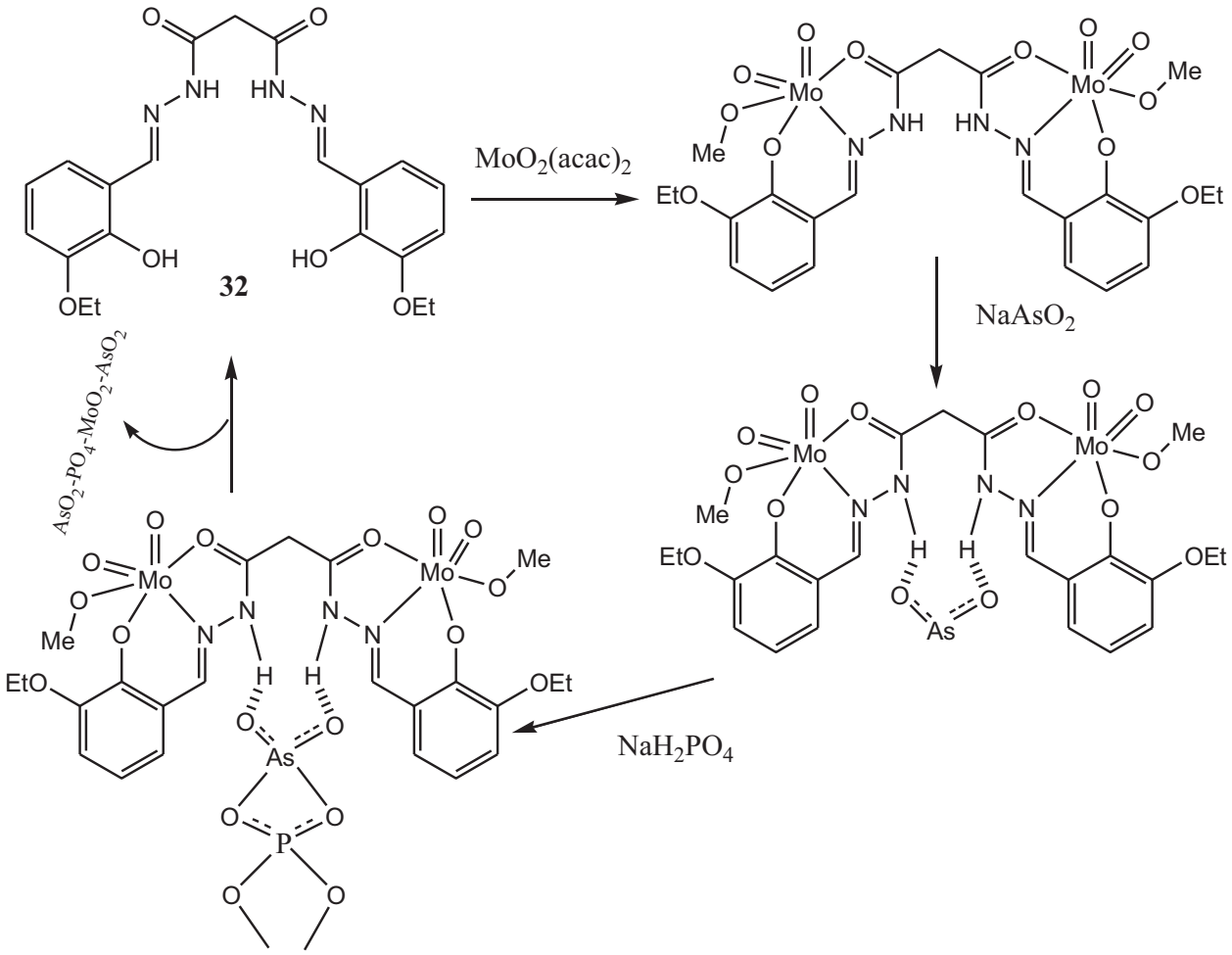

Fig. 20. Chemical structure of chemosensor **32**-Mo(VI) and its proposed sensing mechanism for AsO_2^-.

Murugan et al. synthesized a quinolone-based Zn complex (**34**) for the recognition of AsO_2^- and $H_2PO_4^-$ ions in aqueous DMSO medium (Fig. 22) [121]. Upon addition of $NaAsO_2$ to the Zn-complex solution caused a blue shift in the absorption maximum from 484 to 436 nm along with appearance of new band 505 nm, which contributed to a visible color change from red to yellow that was visible to the naked eye. The Zn-complex presented chelation to AsO_2^- ions and triggered remarkable blue shift in the emission maxima from 650 nm to 566 nm. The complex displayed a good selectivity for AsO_2^- ions with a detection limit of 25 ppb. A 1:1 binding stoichiometry between complex and AsO_2^- was determined by ESI-MS and Job's plot analysis and fluorometric titration exhibited binding constant of 1.1×10^{-3} M for AsO_2^- ion. The efficacy of the complex to image AsO_2^- ion *in vivo* was also illustrated in live zebrafish embryos.

3. Conclusion and perspective

In this review, we have discussed recent interesting reports on arsenic species sensing by several chromogenic and fluorogenic chemosensors and their applications in the detection of arsenic. Here, main attention was given to their strategies in designing, sensing mechanisms and performances and their potential bioimaging applications. We categorized these chemosensors into six types by their sensing strategies, such as (i) during the past decade, chemosensors based on hydrogen-bonding interactions have been extensively employed as sensing mechanisms for the detection of analyte specially anion. In this section, hydrogen-bond donors moiety (like hydroxyl groups, Schiff base, amide and thiourea) containing several chromogenic/fluorogenic probes have been reported by the scientist for the recognition of arsenic ions [92–105]. For the selectivity and sensitivity of these chemosensors, the acidity of the hydrogen atoms and basicity of the anions are very much important. (ii) Additionally, one of the most important signalling mechanism, termed aggregation induced emission (AIE) has also contributed to the analyte detection in recent years. However, only two fluorescent probes with an AIE effect for As^{3+} ion have been mentioned here [107,108]. (iii) Another approach to the detection of analyte (anion, cation or neutral molecule) through the colorimetric-fluorometric technique is the "chemodosimetric approach". This technique includes the specific chemical reaction (generally irreversible) of the target analyte with the molecular probe (chemodosimeter) and is associated with optical properties changes. This chemodosimetric approach is less influenced by the environmental factor and has a distinct benefit in terms of excellent sensitivity, high selectivity and quick response time. In this section, we report a reaction-based probes for As^{3+}. Here, irreversible chemical reaction between chemodosimeter (**22**) and thiophilic As^{3+} ion leads to the formation of highly fluorescent benzothiazole moiety [109]. This chemodosimetric reaction mostly depend on the thiophilic nature of As^{3+} ions. (iv) In addition to the chemodosimetric approach, the metal coordination-based sensing strategy has also been employed for the detection of metal cations. Here, several fluorescent chemosensors have been described primarily on the basis of metal coordination to the oxygen and nitrogen containing probes [111–113]. Besides, one sulphur containing probe is also used to detect arsenic ion *via* this coordination approach [110].

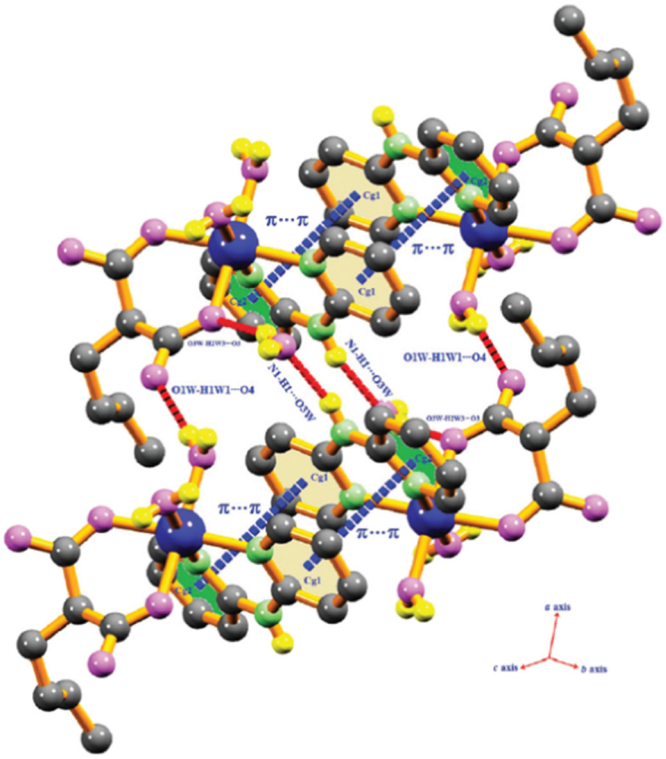

Fig. 21. Crystal packing of the Co(II)-complex. (Here Co = blue, O = pink, N = light green, C = gray, H = yellow) (**33**).
Reproduced from Ref. [120] with permission of The Royal Society of Chemistry.

(v) Due to the high hydration nature of anions, the design and development of fluorescent probes for anions in aqueous media is very difficult. Now, this problem can be solved by using the metal complex displacement strategy, in which a metal cation is displaced from the probe binding pocket in presence of anions, inducing a signal modulation. The above arsenate probe (**27**) is designed based on this displacement strategy [114]. Here, in the presence of AsO_4^{3-}, Al^{3+} is displaced from Al^{3+}-complex (**27**) as more stable aluminum-arsenate ($AlAsO_4$) species (hard acid- hard base combination, HSAB theory) [122–124] and then the fluorescent signals become turn-off. (vi) Transition metal complexes are also employed as chemosensors for the detection of several ions owing to their unique photophysical properties. There are comparatively few reported examples of fluorescent metal complex chemosensors compared to purely organic fluorophore based chemosensors. In this section, one Mn(II) [115], three Cu(II) [116–118], One Mo(VI) [119], One Co(II) [120] and one Zn(II) [121] based chemosensors have been described in detail for the detection of arsenic species *via* different methods.

All these reported chemosensors are associated with changes in the absorption and/or fluorescence intensity or fluorescence quantum yields (Table 1). However, the sensing process of several probes is accompanied by color changes that can be monitored by our naked eye and this will give incredible accessibility for real application. Apart from this one of the authors developed paper based analytical device for arsenic sensing [112]. Due to good cell permeability and low cytotoxic nature, many probes can be used for imaging (*in vitro/in vivo*) arsenic in biological samples. In addition, some probes display ratiometric absorbance/fluorescence behavior toward arsenic sensing. On the other hand, few probes have been also used for detection of arsenic in environment samples with a good detection limit. Again, few probes are able to remove arsenate from drinking water through solid phase extraction method. In some cases, the probe can effectively differentiate between As^{3+} and As^{5+}.

In spite of the recent advancement achieved in this field, there are still many issues.

(i) Water solubility is very important for the practical application of fluorescent chemosensors, specifically for metal cation chemosensors. There are only a few chemosensors that detects arsenic under purely aqueous conditions. However, many of the probes for arsenic only work in organo-aqueous or pure organic solutions, which restricted their real applications. Thus, the invention of novel water-soluble probes will thus support their real applications.

(ii) Although some reported probes exhibit higher sensitivity but they also suffer from interference from other analyte. Therefore, research and development on interference free fluorescent probes for arsenic species detection is still of great interest.

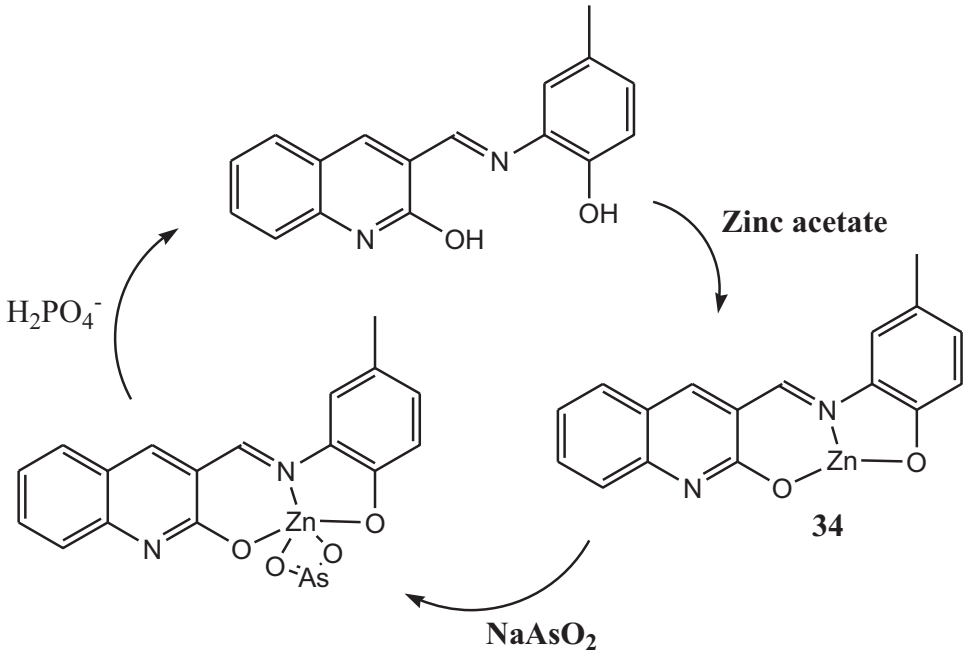

Fig. 22. Chemical structure of chemosensor **34** and its probable sensing mechanism for AsO_2^-.

Table 1
Summary of sensing properties of arsenic chemosensors 1–34.

Probe and analyte/stoichiometry	Probe type/sensing mech.	Medium	$\lambda_{Ex.}$ (nm)	$\lambda_{Em.}$ (nm)	Quantum yield (Φ) in absence/presence of analyte	Limit of detection (LOD)	Binding constant/time	Application	Ref.
1 & $H_2AsO_4^-$/1:1	Turn-on/–	HEPES buffered (0.1 M) solution (methanol/water = 1:4, v/v, pH 7.4)	350	498	0.016/0.196	3×10^{-6} M	8.9×10^3 M^{-1}/–	Live cell imaging	[92]
2 & $H_2AsO_4^-$/1:1	Turn-on/PET, TICT, PICT	HEPES buffered (0.1 M; ethanol–water, 1:99, v/v; pH 7.4) solution	440	532	0.015/0.17	0.001 μM	1.35×10^6 M^{-1}/–	(a) Live cell imaging (b) remove toxic arsenate from drinking water.	[93]
3 & $H_2AsO_4^-$/1:1	Turn-on/–	HEPES buffered (0.1 M; ethanol–water, 1:99, v/v; pH 7.4) solution	400	530	1.6×10^{-2}/21.3×10^{-2}	0.001 μM	1.32×10^4 M^{-1}/–	(a) Live cell imaging (b) remove toxic arsenate from drinking water.	[94]
4 & AsO_3^{3-}/1:1	Turn-on/PET, CHEF	HEPES buffer (1 mM, pH 7.4; water:DMSO (v/v), 9:1) solution	438	532	0.00228/0.01294	54.91 nM (4.12 ppb)	2.5267×10^5 M^{-1}/–	(a) Live cell imaging (b) detection in water samples	[95]
5 & As(III)/–	Colorimetric (ratiometric)	60% ethanol	509↓ to 632↑	–	–	0.26 μM (UV), 25 μM (naked eye for solution), 30 μM (naked eye for resin)	–/3 min. approximately	Detection in water samples	[96]
6 & $H_2AsO_4^-$/2:1	Turn-on/AIEE, CHEF	HEPES buffered (0.1 M, ethanol/water = 1/9, v/v, pH 7.4)	377	540	0.7×10^{-2}/5.3×10^{-2}	5×10^{-9} M	1.38×10^5 $M^{-1/2}$/–	(a) Live cell imaging (b) detection in water samples	[97]
7, **8** & AsO_2^-/1:1	Colorimetric (ratiometric)	5% H_2O-95% DMSO (v/v)	395↓ to 504↑ (**7**) & 407↓ to 534↑ (**8**)	–	–	–	6.12 (**7**), 6.38 (**8**) (Job's method) & 7.42 (**7**), 8.01 (**8**) (molar method)/–	Detection in water samples	[98]
9 & AsO_3^{3-}/1:1	Turn-on/ESIPT	Acetonitrile–water, v/v, 9/1, HEPES buffer, pH 7.2	458	560	0.009/0.315	15 nM	1.0×10^5 M^{-1}/–	Detection in real water samples.	[99]
10 & AsO_2^- $H_2AsO_4^-$/1:1	Turn-on/—	Pure aqueous medium at pH 7.24 (10 mM HEPES buffer, μ = 0.05 M, NaCl).	340	476 (AsO_2^-) & 460 ($H_2AsO_4^-$)	0.031/0.078 (AsO_2^-) & 0.055 ($H_2AsO_4^-$)	0.23 μM (AsO_2^-) & 1.32 μM ($H_2AsO_4^-$)	$(2.80 \pm 0.58) \times 10^4$ M^{-1} for (AsO_2^-) & $(2.03 \pm 0.97) \times 10^5$ M^{-1} for ($H_2AsO_4^-$)/–	Live cell imaging	[100]
11, **12** & AsO_2^-/1:2 (**11**), 1:1 (**12**)	Colorimetric (ratiometric)	DMSO: H_2O (9:1; v/v)	389↓ to 535↑ (**11**) & 380↓ to 507↑ (**12**)	–	–	0.154 ppm (4.97 μM) (**11**) & 0.99 ppm (6.52 μM) (**12**)	6.9×10^5 M^{-1} (**11**) 3.8×10^5 M^{-1} (**12**)/–	–	[101]
13, **14**, **15**, **16** & As (V)/1:2 (**13**), 2:1 (**14**, **15**)	Turn-on/TICT, PICT, PET	DMF/H_2O (v/v, 4:6) (**13**), DMF (**14**, **15**, **16**)	380	550	–	0.88 ppb (**13**), 1.90 ppb (**14**), 2.42 ppb (**15**)	4.26×10^4 M^2 (**13**), 1.93×10^4 $M^{-1/2}$ (**14**), 1.74×10^4 $M^{-1/2}$ (**15**)/20 s	Detection in real water samples	[102]
17 & As(III)/1:1	Colorimetric	H_2O: DMSO (9:1, v/v) & H_2O:	415 to 509	–	–	0.35×10^{-6} M	3.96×10^6 M^{-1}/–	–	[103]

(continued on next page)

Table 1 (*continued*)

Probe and analyte/stoichiometry	Probe type/sensing mech.	Medium	$\lambda_{Ex.}$ (nm)	$\lambda_{Em.}$ (nm)	Quantum yield (Φ) in absence/presence of analyte	Limit of detection (LOD)	Binding constant/time	Application	Ref.
		ACN (9:1, v/v)	(H_2O: DMSO), 397 to 470 (H_2O: ACN)						
18 & $H_2AsO_4^-$/1:1	Turn-on/TICT	HEPES buffer at pH 7.24 in H_2O	340	450	9.8×10^{-3}/11.4×10^{-3}	29 μM	(2.10 ± 0.54) × 10^4 M^{-1}/–	Live cell imaging	[104]
19 & AsO_2^-/1:1	Turn-on/–	DMF: H_2O (HEPES buffer of 7.2 pH, 9:1, v/v)	363	495	–	66 nM DMF: H_2O (9:1, HEPES buffer) & 68 nM DMF: H_2O (9:1)	3.1×10^5 in DMF: H_2O (9:1, HEPES buffer) & 3.2×10^5 in DMF: H_2O (9:1)/–	Detection in real water samples	[105]
20 & As^{3+}/–	Turn-on/AIE	1% THF-distilled water	330	470	–	0.5 ppb	–	–	[107]
21 & As^{3+}/3:1	Turn-on/AIE	THF–water mixtures (v/v, 3/7)	330	455	0.024 (solution), 0.381 (aggregate)/–	1.32 ppb	–	Detection in water samples	[108]
22 & As (III)	Turn-on/ICT	THF	385	496	0.004/0.101	0.53 nM (0.24 ppb)	–	–	[109]
23 & As^{3+}, As^{5+}/1:1	Colorimetric (ratiometric)	DMSO/H_2O (1;1)	480↓ to 580↑	–	–	7.2(As^{3+}) 6.7(As^{5+})	–/<10 sec	–	[110]
24 & As(III)/1:1	Turn-on/–	Acetonitrile: HEPES buffer (4:1, v/v, pH 7.4)	515	555	–	0.164 ppb	0.33×10^6 M^{-1}/–	(a) Detection in waste water samples and (b) live cell imaging	[111]
25 & As^{3+}/1:1	Turn-off/PET	Acetonitrile/aqueous phosphate buffer (8: 2, v/v), pH = 7.2	278	–	–	11.53 nM	7.842×10^8 M^{-1}/–	Detection in waste water samples.	[112]
26 & As^{3+}/2:1	Colorimetric	0.1 M acetate buffer (pH 4.0)	430	–	–	31.8 nM	–	Detection in water samples	[113]
27 & AsO_4^{3-}/–	Turn-off	CH_3OH–HEPES (7/3, v/v)	500	552	–	–	–	–	[114]
28 & $HAsO_4^{2-}$/1:1	Turn-on/–	HEPES buffered (0.1 M) (methanol/water = 0.5/99.5, pH = 7.4)	370	440	1.23×10^{-2}/4.59×10^{-2}	1×10^{-10}M	$3.09 \times 10^3$$M^{-1}$/–	Live cell imaging	[115]
29 & As^{3+}/–	Turn-on/–	Water	310	350	–	–	–	–	[116]
30 & As(III)/–	Turn-on/–	Aqueous solution	250	380	–	49.75 fM	–	Live cell imaging	[117]
31 & As^{5+}/1:2	Turn-on/PET	Aqueous solution	497	600	0.032/0.344	26 nM	8.50×10^8 M^{-2}/–	(a) Live cell imaging and (b) detection in water samples	[118]
32 & AsO_2^-/1:1	Turn-on/ratiometric	DMSO/H_2O (4/1, v/v, pH 7.4)	336	393↓ to 494↑	0.156/0.632	1.2×10^{-10} M	6.49×10^4 M^{-1}/–	(a) Detection in water samples, (b) remove arsenate from water by solvent extraction method	[119]
33 & As(III)/–	Turn-on/–	Aqueous solution	315	350	0.019/0.477	0.49 μM	–	Intracellular tracking of arsenic bacterial systems	[120]
34 & AsO_2^-/1:1	Turn-on/ICT	Aqueous DMSO	390	566	–	25 ppb	1.1×10^{-3} M/–	Imaging (*in vivo*) in live zebrafish embryos	[121]

(iii) In addition, two probes show "turn-off"fluorescence toward arsenic sensing. However, "turn-on"probes will be more effective, sensitive and accurate for the detection of analytes. It will be another significant direction of research.

(iv) The reaction-based chemosensors *i.e.* chemodosimeters have been regarded as a useful approach regarding the selectivity and sensitivity issues. Nevertheless, only one example discussed here demonstrate chemodosimetric nature, which is a limitation in this field.

(v) Here, most of the reported fluorescent probes are based on emission intensity. Though intensity-based probes are highly sensitive toward analytes owing to the lack of background signal, a significant disadvantage is that emission intensity measurements may be affected by several external environmental factors such as temperature, pH, unknown concentration of analytes, solvent polarity, draft of light source *etc*. By contrast, ratiometric fluorescent probes are extremely effective, as they permit the measurement of emission intensities at two distinct wavelengths, which allows a built-in rectification of environmental factors as well as enhancing the dynamic range of emission measurements. Ratiometric probes thus allows to obtain more precise and quantitative results not only in solution phase but also in biological systems. Hence, development of novel ratiometric probes for arsenic ions should be of main objective for the future of research in this area.

(vi) Several sensing mechanisms such as PET, CHEF, TICT, PICT, ICT, AIE and ESIPT have been discussed in this review. However, other photophysical mechanisms like FRET (fluorescence resonance energy transfer), TBET (through bond energy transfer), C═N isomerization and monomer–excimer formation should also be explored in near future.

(vii) However, although several chemosensors for arsenic have been reported by chemists and also applied in biological studies but a big challenge persists to develop NIR-based fluorescent chemosensors/chemodosimeters. NIR-based fluorescent chemosensors/chemodosimeters act as an effective tool for imaging and tracking of different biological specimens *in vitro* and *in vivo* owing to their profound tissue penetration strength with nominal damage and least interference from the background auto fluorescence of indigenous biomolecules present in living systems. Moreover, another efficient and increasingly popular method, namely time-gated luminescence technique (TGL) using long lived luminescent probes could be the most promising technology for the detection and imaging of the analyte at subcellular, cellular and molecular levels because it allows a specific way to remove the background autofluorescence and light scattering for background-free analysis [125,126].

The future study in this area should therefore be aimed toward the development of novel highly selective and sensitive arsenic probes with simple synthetic route, anti-interference, rapid response, low detection limit, large stokes shift, high quantum yield, good water solubility, photostability and strong biological compatibility.

We believe that this review will encourage scientists to explore novel fluorometric/colorimetric chemosensors/chemodosimeters for the detection of arsenic along with innovative applications.

Declaration of competing interest

The authors declare no conflict of interest for this manuscript.

Acknowledgements

DB thanks CSIR, New Delhi, India for a fellowship. SKM would like to thank Mr. Soumendra Nath Manna and Dr. Sanchita Mondal for their help in preparing the graphical abstract.

References

[1] D. Harper, "Arsenic". Online Etymology Dictionary.
[2] B.K. Mandal, K.T. Suzuki, Arsenic round the world: a review, Talanta. 58 (2002) 201.
[3] H. Kaur, R. Kumar, J.N. Babu, S. Mittal, Advances in arsenic biosensor development – a comprehensive review, Biosens. Bioelectron. 63 (2015) 533.
[4] W.R. Cullen, K.J. Reimer, Arsenic speciation in the environment, Chem. Rev. 89 (1989) 713.
[5] S. Shen, X.-F. Li, W.R. Cullen, M. Weinfeld, X.C. Le, Arsenic binding to proteins, Chem. Rev. 113 (2013) 7769.
[6] J.O. Nriagu, Arsenic in the Environment: Part I, Advances in Environmental Science and Technology, John Wiley & Sons, New York, 1994.
[7] N. Bhandari, R. J. Reeder, D. R. Strongin, Photoinduced oxidation of arsenite to arsenate in the presence of goethite, Environ. Sci., Technol. 46 (2012) 8044.
[8] H. A. Tourtelot, Geochem. Minor-element composition and organic carbon content of marine and nonmarine shales of Late Cretaceous age in the western interior of the United States, Cosmochim. Acta, 28 (1964) 1579.
[9] A. Basu, D. Saha, R. Saha, T. Ghosh, B. Saha, A review on sources, toxicity and remediation technologies for removing arsenic from drinking water, Res. Chem. Intermed. 40 (2014) 447.
[10] B. Sadee, M.E. Foulkes, S.J. Hill, Coupled techniques for arsenic speciation in food and drinking water: a review, J. Anal. At. Spectrom. 30 (2015) 102.
[11] C. K. Jain, I. ALI, arsenic: occurrence, toxicity and speciation techniques, Wat. Res. 34 (2000) 4304.
[12] P. L. Smedley, D.G. Kinniburgh, Source and Behaviour of Arsenic in Natural Waters, British Geological Survey, U.K., (Chapter 1).
[13] K. Ohnishi, H. Yoshida, K. Shigeno, S. Nakamura, S. Fujisawa, K. Naito, K. Shinjo, Y. Fujita, H. Matsui, A. Takeshita, S. Sugiyama, H. Satoh, H. Terada, R. Ohno, Prolongation of the QT interval and ventricular tachycardia in patients treated with arsenic trioxide for acute promyelocytic leukemia, Ann. Intern. Med. 133 (2000) 881.
[14] W.T. Frankenberger Jr., Environmental Chemistry of Arsenic, Marcel Dekker, Inc., New York, 2002.
[15] V.K. Gupta, A. Nayak, S. Agarwal, R. Dobhal, D.P. Uniyal, P. Singh, B. Sharma, S. Tyagi, R. Singh, Arsenic speciation analysis and remediation techniques in drinking water, Desalin. Water Treat. 40 (2012) 231.
[16] J.G. Webster, in: C.P. Marshall, R.W. Fairbridge (Eds.), Encyclopedia of Geochemistry, Chapman Hall, London 1999, p. 21.
[17] P.L. Smedley, D.G. Kinniburgh, A review of the source, behaviour and distribution of arsenic in natural waters, Appl. Geochem. 17 (2002) 517.
[18] R.K. Zalups, D.J. Koropatnick, Molecular Biology and Toxicology of Metals, CRC Press, Taylor and Francis Group, 2000.
[19] T.M. Clancy, K.F. Hayes, L. Raskin, Arsenic waste management: a critical review of testing and disposal of arsenic-bearing solid wastes generated during arsenic removal from drinking water, Environ. Sci. Technol. 47 (2013) 10799.
[20] D. Merulla, N. Buffi, S. Beggah, F. Truffer, M. Geiser, P. Renaud and J. R. Meer, Bioreporters and biosensors for arsenic detection. Biotechnological solutions for a world-wide pollution problem, Curr. Opin. Biotech. 24 (2013) 534.
[21] D. Richardson, T.A. Ternes, Water analysis: emerging contaminants and current issues, Anal. Chem. 77 (2005) 3807.
[22] D. Cantzos, D. Nikolopoulos, Identifying long-memory trends in pre-seismic MHz disturbances through support vector machines, J. Earth Sci. Clim. Change. 6 (2015) 1.
[23] K. Nocon, W. Rogula-Kozłowska, K. Widziewicz, Research on Chromium and Arsenic Speciation in Atmospheric Particulate Matter: Short Review, EDP Sciences, 2018, p. 01026.
[24] X.-Y. Yu, T. Luo, Y. Jia, Y.-X. Zhang, J.-H. Liu, X.-J. Huang, Porous hierarchically micro-/nanostructured MgO: morphology control and their excellent performance in As(III) and As(V) removal, J. Phys. Chem. C 115 (2011) 22242.
[25] V.J. Sachin, B. Eugenio, D.Y. Ganapati, K.R. Virendra, O. Inmaculada, V.M. Kumudini, Arsenic and fluoride contaminated groundwaters: a review of current technologies for contaminants removal, J. Environ. Manag. 162 (2015) 306.
[26] E. Munoz, S. Palmero, Analysis and speciation of arsenic by stripping potentiometry: a review, Talanta. 65 (2005) 613.
[27] D. Sutherland, P.M. Swash, A.C. Macqueen, L.E. McWilliam, D.J. Ross, S.C. Wood, A field based evaluation of household arsenic removal technologies for the treatment of drinking water, Environ. Technol. 23 (2002) 1385.
[28] P.L. Smedley, D.G. Kinniburgh, A review of the source, behaviour and distribution of arsenic in natural waters, Appl. Geochem. 17 (2002) 517.
[29] M.J. Watts, M. Button, J.O. Reill, A.L. Marcilla, R.A. Shaw, N.I. Ward, Field based speciation of arsenic in UK and Argentinean water samples, Environ. Geochem. Health 32 (2010) 479.
[30] M. Asadollahzadeh, N. Niksirat, H. Tavakoli, A. Hemmati, P. Rahdari, M. Mohammadi, R. Fazaeli, Application of multi-factorial experimental design to successfully model and optimize inorganic arsenic speciation in environmental water samples by ultrasound assisted emulsification of solidified floating organic drop microextraction, Anal. Methods 6 (2014) 2973.
[31] K.H. Morales, L. Ryan, T.L. Kuo, M.M. Wu, C.J. Chen, Risk of internal cancers from arsenic in drinking water, Environ. Health Perspect. 108 (2000) 655.
[32] R. Stone, Arsenic and paddy rice: a neglected cancer risk? Science 321 (2008) 184.
[33] U.K. Chowdhury, B.K. Biswas, T.R. Chowdhury, G. Samanta, B.K. Mandal, G.C. Basu, C.R. Chanda, D. Lodh, K.C. Saha, S.K. Mukherjee, Groundwater arsenic contamination in Bangladesh and West Bengal, India, Environ. Health Perspect. 108 (2000) 393.

[34] P. Williams, M. Islam, E. Adomako, A. Raab, S. Hossain, Y. Zhu, J. Feldmann, A. Meharg, Increase in rice grain arsenic for regions of Bangladesh irrigating paddies with elevated arsenic in groundwaters, Environ. Sci. Technol. 40 (2006) 4903.
[35] Y.G. Zhu, P.N. Williams, A.A. Meharg, Exposure to inorganic arsenic from rice: a global health issue? Environ. Pollut. 154 (2008) 169.
[36] World Health Organisation, Guidelines for Drinking Water Quality, 1993, p. 41.
[37] M. Bissen, F. H. Frimmel, Arsenic – a Review. Part I: Occurrence, Toxicity, Speciation, Mobility, Acta Hydrochim. Hydrobiol. 31 (2003) 9.
[38] M. Vahter, Metabolism of arsenic, in: B.A. Fowler (Ed.), Biological and Environmental Effects of Arsenic, Elsevier, Amsterdam 1983, pp. 171–198.
[39] A.H. Hall, Chronic arsenic poisoning, Toxicol. Lett. 128 (2002) 69.
[40] J.T. Hindmarsh, R.F. Mc Curdy, Clinical and environmental aspects of arsenic toxicity, CRC Crit. Rev. Clin. Lab. Sci. 23 (1986) 315.
[41] S. C. Mukherjee, Murshidabad-one of the nine groundwater arsenic-affected districts of West Bengal, India. part II: dermatological, neurological, and obstetric findings, Clin Toxicol. 43 (2005) 835.
[42] D. Mohan, C.U. Pittman Jr., Arsenic removal from water/wastewater using adsorbents—a critical review, J. Hazard. Mater. 142 (2007) 1.
[43] I.A. Katsoyiannis, M. Mitrakas, I.A. Zouboulis, Arsenic occurrence in Europe: emphasis in Greece and description of the applied full-scale treatment plants, Desalin. Water Treat. 54 (2015) 2100.
[44] P. Sarkar, S. Banerjee, D. Bhattacharyay, A.P.F. Turner, Electrochemical sensing systems for arsenate estimation by oxidation of L-cysteine, Ecotoxicol. Environ. Saf. 73 (2010) 1495.
[45] S. Kapaj, H. Peterson, K. Liber and P. Bhattacharya, Human health effects from chronic arsenic poisoning – a review, J. Environ. Sci. Health, Part A: Toxic/Hazard. Subst. Environ. Eng., 41 (2006) 2399.
[46] P.B. Tchounwou, A.K. Patlolla, J.A. Centeno, Carcinogenic and systemic health effects associated with arsenic exposure – a critical review, Toxicol. Pathol. 31 (2003) 575.
[47] E.S. Hansen, Shared risk factors for cancer and atherosclerosis – a review of the epidemiological evidence, Mutat. Res. 239 (1990) 163.
[48] C.J. Chen, Y.M. Hsueh, M.S. Lai, M.P. Shyu, S.Y. Chen, M.M. Wu, T.L. Kuo, T.Y. Tai, Increased prevalence of hypertension and long-term arsenic exposure, Hypertens. 25 (1995) 53.
[49] C.J. Chen, H.Y. Chiou, M.H. Chiang, L.J. Lin, T.Y. Tai, Dose-response relationship between ischemic heart disease mortality and long-term arsenic exposure, Arterioscler. Thromb. Vasc. Biol. 16 (1996) 504.
[50] W.R. Chappell, C.O. Abernathy, R.L. Calderon, Arsenic Exposure and Health Effects, first ed. Elsevier Science, London, 1999.
[51] T. Yoshida, H. Yamamuchi, G.F. Sun, Chronic health effects in people exposed to arsenic via the drinking water: dose–response relationships in review, Toxicol. Appl. Pharmacol. 198 (2004) 243.
[52] A. H. Smith, C. Hopenhayn-Rich, M. N. Bates, H. M. Goeden, I. H. Picciotto, H. M. Duggan, R. W. Michael, J. Kosnett, M. T. Smith, Cancer risks from arsenic in drinking water, Environ. Health Perspect. 97 (1992) 259.
[53] C.J. Chen, Y.M. Hsueh, M.S. Lai, M.P. Shyu, S.Y. Chen, M.M. Wu, T.L. Kuo, T.Y. Tai, Increased prevalence of hypertension and long-term arsenic exposure, Hypertension 25 (1995) 53.
[54] J. Balasubramanian, A. Kumar, Study of effect of sodium arsenite on lipid metabolism of Heteropneustes fossilis and the chelating effect of zeolite, Adv. Biosci. Bioeng. 1 (2013) 22.
[55] E.J. Henriksen, J.O. Holloszy, Effects of phenylarsine oxide on stimulation of glucose transport in rat skeletal muscle, Am. J. Phys. 258 (1990) C648.
[56] C. K. Jain, I. Ali, arsenic: occurrence, toxicity and speciation techniques, Water Res. 34 (2000) 4304.
[57] A.M. Spuches, H.G. Kruszyna, A.M. Rich, D.E. Wilcox, Thermodynamics of the As(III)−thiol interaction: arsenite and monomethylarsenite complexes with glutathione, dihydrolipoic acid, and other thiol ligands, Inorg. Chem. 44 (2005) 2964.
[58] Some metals and metallic compounds, IARC Monogr. Eval. Carcinog. Risk Chem. Hum., 1980, vol. 23.
[59] Priority list of hazardous substances, http://www.atsdr.cdc.gov/spl/index.html.
[60] M.A. Ferreira, A.A. Barros, Determination of As(III) and arsenic(V) in natural waters by cathodic stripping voltammetry at a hanging mercury drop electrode, Anal. Chim. Acta 459 (2002) 151.
[61] M. Kopanica, L. Norotny, Determination of traces of arsenic(III) by anodic stripping voltammetry in solutions, natural waters and biological material, Anal. Chim. Acta 368 (1998) 211.
[62] M. Boadu, E.K. Osae, A.A. Golow, Y.S. Armah, B.J.B. Nyarko, Determination of arsenic in some water bodies, untreated ore and tailing samples at Konongo in the Ashanti region of Ghana and its surrounding towns and villages by instrumental neutron activation analysis, J. Radioanal. Nucl. Chem. 249 (2001) 581.
[63] N. Izumi, B. Yukari, T. Keiichi, N. Satoshi, H. Minako, H. Akiko, H. Yoshikazu, X-ray microanalysis of biological samples by high-resolution energy dispersive microcalorimeter spectrometer using a low-voltage scanning electron microscope, Chem. Lett. 37 (2008) 304.
[64] K. Anezaki, I. Nukatsuka, K. Ohzeki, determination of arsenic (III) and total arsenic (III,V) in water samples by resin suspension graphite furnace atomic absorption spectrometry, Anal. Sci. 15 (1999) 829.
[65] M.M. Gomez, M. Kovecs, M.A. Palacios, I. Pizarro, C. Camara, Effect of the mineralization method on arsenic determination in marine organisms by hydride generation atomic fluorescence spectroscopy, Microchim. Acta 150 (2005) 9.
[66] E. Sanz, R. Munoz-Olivas, C. Camara, M. K. Sengupta, S. Ahamed, Arsenic speciation in rice, straw, soil, hair and nails samples from the arsenic-affected areas of Middle and Lower Ganga plain, J. Environ. Sci. Health, Part A. 42 (2007) 1695.
[67] G. Alvarez-Llamas, M.R. de la Campa, A. SanzMedel, An alternative interface for CE–ICP–MS cadmium speciation in metallothioneins based on volatile species generation, Anal. Chim. Acta 546 (2005) 236.
[68] U. Kohlmeyer, E. Jantzen, J. Kuballa, S. Jakubik, Benefits of high resolution IC–ICP–MS for the routine analysis of inorganic and organic arsenic species in food products of marine and terrestrial origin, Anal. Bioanal. Chem. 377 (2003) 6.
[69] B.K. Jena, C.R. Raj, Gold nanoelectrode ensembles for the simultaneous electrochemical detection of ultratrace arsenic, mercury, and copper, Anal. Chem. 80 (2008) 4836.
[70] Y. Wu, S. Zhan, F. Wang, L. He, W. Zhi, P. Zhou, Cationic polymers and aptamers mediated aggregation of gold nanoparticles for the colorimetric detection of arsenic(III) in aqueous solution, Chem. Commun. 48 (2012) 4459.
[71] Y. Wu, L. Liu, S. Zhan, F. Wang, P. Zhou, Ultrasensitive aptamer biosensor for arsenic (III) detection in aqueous solution based on surfactant-induced aggregation of gold nanoparticles, Analyst 137 (2012) 4171.
[72] D. Melamed, Monitoring arsenic in the environment: a review of science and technologies with the potential for field measurements, Anal. Chim. Act. 532 (2005) 1.
[73] L. Wu, C. Huang, B.P. Emery, A.C. Sedgwick, S.D. Bull, X.-P. He, H. Tian, J. Yoon, J.L. Sessler, T.D. James, Fo¨rster resonance energy transfer (FRET)-based small-molecule sensors and imaging agents, Chem. Soc. Rev. 49 (2020) 5110.
[74] S.K. Manna, A. Gangopadhyay, K. Maiti, S. Mondal, A.K. Mahapatra, Recent developments in fluorometric and colorimetric chemodosimeters targeted towards hydrazine sensing: present success and future possibilities, ChemistrySelect 4 (2019) 7219.
[75] A.P. Demchenko, Introduction to Fluorescence Sensing, Springer, New York, 2008.
[76] T.L. Mako, J.M. Racicot, M. Levine, Supramolecular luminescent sensors, Chem. Rev. 119 (2019) 322.
[77] J. Yan, S. Lee, A. Zhang, J. Yoon, Self-immolative colorimetric, fluorescent and chemiluminescent chemosensors, Chem. Soc. Rev. 47 (2018) 6900.
[78] D. Wu, A.C. Sedgwick, T. Gunnlaugsson, E.U. Akkaya, J. Yoon, T.D. James, Fluorescent chemosensors: the past, present and future, Chem. Soc. Rev. 46 (2017) 7105.
[79] S. Antonova, E. Zakharova, Inorganic arsenic speciation by electroanalysis. From laboratory to field conditions: a mini-review, Electrochem. Commun. 70 (2016) 33.
[80] S. Kempahanumakkagari, A. Deep, K.-H. Kim, S.K. Kailasa, H.-O. Yoon, Nanomaterial-based electrochemical sensors for arsenic - a review, Biosens. Bioelectron. 95 (2017) 106.
[81] D.Q. Hung, O. Nekrassova, R.G. Compton, Analytical methods for inorganic arsenic in water: a review, Talanta 64 (2004) 269.
[82] D. Merulla, N. Buffi, S. Beggah, F. Truffer, M. Geiser, P. Renaud, J.R. van der Meer, Bioreporters and biosensors for arsenic detection, Biotechnological solutions for a world-wide pollution problem Curr. Opin. Biotechnol. 24 (2013) 534.
[83] H. Kaur, R. Kumar, J.N. Babu, S. Mittal, Advances in arsenic biosensor development - a comprehensive review, Biosens. Bioelectron. 63 (2015) 533.
[84] L. S. B. Upadhyay, N. Kumar, S. Chauhan, Minireview: whole-cell, nucleotide, and enzyme inhibition-based biosensors for the determination of arsenic, Anal. Lett. 51 (2017)1265.
[85] J. Hao, M.-J. Han, S. Han, X. Meng, T.-L. Su, Q.K. Wang, SERS detection of arsenic in water: a review, J. Environ. Sci. 36 (2015) 152.
[86] N. Yogarajah, S.S.H. Tsai, Detection of trace arsenic in drinking water: challenges and opportunities for microfluidics, Environ. Sci. Water Res. Technol. 1 (2015) 426.
[87] B. Sadee, M.E. Foulkes, S.J. Hill, Coupled techniques for arsenic speciation in food and drinking water: a review, J. Anal. At. Spectrom. 30 (2015) 102.
[88] J. Ma, M.K. Sengupta, D. Yuan, P.K. Dasgupta, Speciation and detection of arsenic in aqueous samples: a review of recent progress in non-atomic spectrometric methods, Anal. Chim. Acta 831 (2014) 1.
[89] Q. Liu, X. Lu, H. Peng, A. Popowich, J. Tao, J.S. Uppal, X. Yan, D. Boe, X.C. Le, Speciation of arsenic - a review of phenylarsenicals and related arsenic metabolites, Trends Anal. Chem. 104 (2018) 171.
[90] L. Zhang, X.- R. Chen, S. -H. Wen, R. -P. Liang, J. -D. Qiu Optical sensors for inorganic arsenic detection Trends Ana. Chem. 118 (2019) 869.
[91] P. Devi, A. Thakur, R.Y. Lai, S. Saini, R. Jain, Praveen Kumar d, Progress in the materials for optical detection of arsenic in water, Trends Ana. Chem. 110 (2019) 97.
[92] S. Lohar, A. Sahana, A. Banerjee, A. Banik, S.K. Mukhopadhyay, J.S. Matalobos, D. Das, Antipyrine based arsenate selective fluorescent probe for living cell imaging, Anal. Chem. 85 (2013) 1778.
[93] A. Banerjee, A. Sahana, S. Lohar, S. Panja, S.K. Mukhopadhyay, D. Das, Visible light excitable fluorescence probe and its functionalized Merrifield polymer: selective sensing and removal of arsenate from real samples, RSC Adv. 4 (2014) 3887.
[94] S. Nandi, A. Sahana, B. Sarkar, S.K. Mukhopadhyay, D. Das, Pyridine based fluorescence probe: simultaneous detection and removal of arsenate from real samples with living cell imaging properties, Journal Fluorescence 25 (2015) 1191.
[95] S. Lohar, S. Pal, B. Sen, M. Mukherjee, S. Banerjee, P. Chattopadhyay, Selective and sensitive turn-on chemosensor for arsenite ion at ppb level in aqueous media applicable in cell staining, Anal. Chem. 86 (2014) 11357.
[96] S. Sirawatcharin, A. Saithongdee, A. Chaicham, B. Tomapatanaget, A. Imyim, N. Praphairaksit, Naked-eye and colorimetric detection of arsenic(III) using difluoroboron-curcumin in aqueous and resin bead support systems, Anal. Sci. 30 (2014) 1129.
[97] A. Sahana, A. Banerjee, S. Lohar, S. Panja, S.K. Mukhopadhyay, J.S. Matalobos, D. Das, Fluorescence sensing of arsenate at nanomolar level in a greener way: naphthalene based probe for living cell imaging, Chem.Commun. 49 (2013) 7231.
[98] N. Gupta, A.K. Singh, S. Bhardwaj, D. Singhal, Electroanalytical studies of chromone based ionophores for the selective determination of arsenite ion, Electroanal. 27 (2015) 1166.

[99] R. Purkait, S. Maity, C. Sinha, A hydrazine-based thiocarbamide probe for colorimetric and turn-on fluoremetric detection of PO_4^{3-} and AsO_3^{3-} in semi-aqueous medium, New J. Chem. 42 (2018) 6236.
[100] A. S. M. Islam, R. Alam, A. Katarkar, K. Chaudhuri, M. Ali, Di-oxime based selective fluorescent probe for arsenate and arsenite ions in a purely aqueous medium with living cell imaging applications and H-bonding induced microstructure formation, Analyst 140 (2015) 2979.
[101] A. Singh, M. Mohan, D. R. Trivedi, Design and synthesis of malonohydrazide based colorimetric receptors for discrimination of maleate over fumarate and detection of F^-, AcO^- and AsO_2^- ions, Spectrochim. Acta A 229 (2020) 117883.
[102] L. Wang, Y. Li, X. Tian, C. Yang, L. Lu, Z. Zhou, Y. Huang, Y. Nie, Construction of salicylaldehyde analogues as turn-on fluorescence probes and their electronic effect on sensitive and selective detection of As(V) in groundwater, Anal. Methods 11 (2019) 955.
[103] A. Deepa, V. Padmini, Highly efficient colorimetric sensor for selective and sensitive detection of arsenite ion (III) in aqueous medium, J. Fluoresc. 29 (2019) 813.
[104] M. Dolai, R. Alam, A. Katarkar, K. Chaudhuri, M. Ali, Oxime based selective fluorescent sensor for arsenate ion in a greener way with bio-imaging application, Anal. Sci. 32 (2016) 1295.
[105] N. Yadav, A.K. Singh, Dual anion colorimetric and fluorometric sensing of arsenite and cyanide ions, RSC Adv. 6 (2016) 100136.
[106] J. Luo, Z. Xie, J.W.Y. Lam, L. Cheng, H. Chen, C. Qiu, H.S. Kwok, X. Zhan, Y. Liu, D. Zhu, B.Z. Tang, Aggregation-induced emission of 1-methyl-1,2,3,4,5-pentaphenylsilole, Chem. Commun. 18 (2001) 1740.
[107] M. Baglan, S. Atılgan, Selective and sensitive turn-on fluorescent sensing of arsenite based on cysteine fused tetraphenylethene with AIE characteristics in aqueous media, Chem.Commun. 49 (2013) 5325.
[108] X. Tian, L. Chen, Y. Li, C. Yang, Y. Nie, C. Zhou, Y. Wang, Design and synthesis of molecule with aggregation-induced emission effect and its application in detection of arsenite in groundwater, J. Mater. Chem. 5 (2017) 3669.
[109] V.C. Ezeh, T.C. Harrop, A sensitive and selective fluorescence sensor for the detection of arsenic(III) in organic media, Inorg. Chem. 51 (2012) 1213.
[110] K. Chauhan, P. Singh, B. Kumari, R.K. Singhal, Synthesis of new benzothiazole schiff base as selective and sensitive colorimetric sensor for arsenic on-site detection at ppb level, Anal. Methods 9 (2017) 1779.
[111] S. Paul, S. Bhuyan, S.K. Mukhopadhyay, N.C. Murmu, P. Banerjee, Sensitive and selective in vitro recognition of biologically toxic As(III) by rhodamine based chemoreceptor, ACS Sustain. Chem. Eng. 7 (2019) 13687.
[112] P.G. Sutariya, H. Soni, S.A. Gandhib, A. Pandya, Single-step fluorescence recognition of As^{3+}, Nd^{3+} and Br^- using pyrene-linked calix[4]arene: application to real samples, computational modelling and paper-based device, New J. Chem. 43 (2019) 737.
[113] J.-H. Park, G. Yeom, D. Hong, E.-J. Jo, C.-J. Park, M.-G. Kim, A simple and label-free detection of As^{3+} using 3-nitro-l-tyrosine as an As^{3+}-chelating ligand, Sensors. 19 (2019) 2857.
[114] S. Dey, S. Sarkar, D. Maity, P. Roy, Rhodamine based chemosensor for trivalent cations: synthesis, spectral properties, secondary complex as sensor for arsenate and molecular logic gates, Sensors Actuators B Chem. 246 (2017) 518.
[115] S. Das, A. Banerjee, S. Lohar, B. Sarkar, S.K. Mukhopadhyay, J.S. Matalobos, A. Sahana, D. Das, 2-(2-Pyridyl) benzimidazole based ternary Mn(II) complex as arsenate selective turn-on fluorescence probe: ppb level determination and cell imaging studies, New J. Chem. 38 (2014) 2744.
[116] B. Dey, R. Saha, P. Mukherjee, A luminescent-water soluble inorganic co-crystal for a selective pico-molar range arsenic(III) sensor in water medium, Chem. Commun. 49 (2013) 7064.
[117] B. Dey, P. Mukherjee, R.K. Mondal, A.P. Chattopadhyay, I. Hauli, S.K. Mukhopadhyay, M. Fleck, Femtomolar level sensing of inorganic arsenic (III) in water and in livingsystems by a non-toxic fluorescent probe, Chem. Commun. 50 (2014) 15263.
[118] M. Venkateswarulu, D. Gambhir, H. Kaur, P.V. Daniel, P. Mondal, R.R. Koner, A long-range emissive mega-Stokes inorganic–organic hybrid material with peripheral carboxyl functionality for As(V) recognition and its application in bioimaging, Dalton Trans. 46 (2017) 13118.
[119] M. Banerjee, S. Ta, M. Ghosh, A. Ghosh, D. Das, Sequential fluorescence recognition of molybdenum(VI), arsenite, and phosphate ions in a ratiometric manner: a facile approach for discrimination of AsO_2^- and $H_2PO_4^-$, ACS Omega 4 (2019) 10877.
[120] S. Dhibar, P. Yadav, T. Paul, K. Sarkar, A.P. Chattopadhyay, A. Krawczuk, B. Dey, A bio-relevant supramolecular Co(II)-complex for selective fluorescent sensor of μM range inorganic As(III) in water medium and its intracellular tracking in bacterial systems, Dalton Trans. 48 (2019) 4362.
[121] A.S. Murugan, N. Vidhyalakshmi, U. Ramesh, J. Annaraj, In vivo bio-imaging of sodium meta-arsenite and hydrogen phosphate in zebrafish embryos using red fluorescent zinc complex, Sensors Actuators B Chem. 281 (2019) 507.
[122] R.G. Pearson, Hard and soft acids and bases, HSAB, part 1: fundamental principles, J. Chem. Edu. 45 (1968) 581.
[123] R.G. Pearson, Hard and soft acids and bases, HSAB, part II: underlying theories J, Chem. Edu. 45 (1968) 643.
[124] F. L. Pantuzzo, L. R.G. Santos, V. S.T. Ciminelli, Solubility-product constant of an amorphous aluminum-arsenate phase (AlAsO4·3.5H2O) AT 25 °C, Hydrometallurgy 144–145 (2014) 63.
[125] K. Y. Zhang, Q Yu, H. Wei, S Liu, Q Zhao, W Huang, Long-lived emissive probes for time-resolved photoluminescence bioimaging and biosensing, Chem. Rev. 118 (2018), 1770.
[126] R. Zhang, J. Yuan, Responsive metal complex probes for time-gated luminescence biosensing and imaging, Acc. Chem. Res. 53 (2020) 1316.